



Analysis and Review of Near-Nozzle Mixing in Extrusion-Based Additive Manufacturing of Concrete: Advancing Cross-Sectional Image Analysis Techniques for Enhanced Homogeneity and Quality Assessment

Academic Thesis for the Acquisition of the Degree
M.Sc.

at the Faculty of Mechanical Engineering Technical University of Munich

Subject Supervisor Prof. Dr.-Ing. Johannes Fottner
Chair of Materials Handling, Material Flow, Logistics

Supervisor M.Sc. Maximilian Dahlenburg

Submitted by Han Li

Submitted on: 16.04.2024 in Garching

Inventory No. FML: 2023071

Table of Contents

Table of Contents	III
List of Abbreviations	VII
List of symbols	IX
1 Introduction	1
1.1 Motivation	1
1.2 Objective	2
2 State of the Art	3
2.1 Additive Manufacturing (AM)	3
2.2 3D Concrete Printing (3DCP)	6
2.2.1 Particle-Bed 3D Printing	8
2.3 Extrusion-Based 3D Concrete Printing (E3DCP)	9
2.3.1 Digital concrete processing	11
2.3.2 Shotcrete-based 3D printing (SC3DP)	14
2.3.3 Multi-Material Additive Manufacturing (MMAM)	15
2.3.4 Collaborative Research Centre TRR277 AMC and Project A03	17
2.3.5 Near-Nozzle-Mixing (NNM)	18
2.3.6 Gradation-Ready Extrusion System (GRES)	19
2.3.7 Material and Recipe	20
2.4 Homogeneity Analysis	22
2.4.1 Definition of Homogeneity	23
2.4.2 Methods of Homogeneity Analysis	23
2.4.3 Statistical Methods for Homogeneity Evaluation	24

2.5	Programming Methodology	25
2.5.1	Python	26
2.5.2	Jupyter Notebook	26
2.5.3	Useful Libraries	27
2.6	Image Analysis Techniques	28
2.6.1	Grayscale Conversion	28
2.6.2	Noise Reduction	29
2.6.3	Thresholding Methods	30
2.6.4	Morphological Operation	32
3	Analysis and Classification of NNM in AM for Concrete Construction	33
4	Homogeneity Analysis and Mix Quality Evaluation in NNM with GRES V1.3	35
4.1	Experimental Procedure	35
4.1.1	Mixing Proportioning	37
4.1.2	Primary Mixing	39
4.1.3	Storage	39
4.1.4	Transport and Secondary Mixing	41
4.2	Sample Preparation	42
4.2.1	Sample Collection	42
4.2.2	Sample Processing	43
4.2.3	Cross-Sectional Image Acquisition	45
4.3	Image Processing	46
4.3.1	Image Preprocessing	47
4.3.2	Image Segmentation	49

4.3.3 Image Processing Validation	51
4.4 Statistical Analysis	52
4.4.1 Implementation of Statistical Analysis of Area Fractions	52
4.4.2 Validation of the Statistical Analysis	56
4.5 Interpretation of the Results	58
5 Summary	61
6 Limitations and Outlook	63
Bibliography	65
List of Figures	71
List of Tables	1
A Appendix	A-1
B Appendix	1

List of Abbreviations

Abbreviation	Meaning
3DCP	3D concrete printing
E3DCP	Extrusion-based 3D concrete printing
AM	Additive manufacturing
NNM	Near-nozzle mixing
GRES	Gradation-ready extrusion system
LWM	Light weight mortar
AMC	Additive manufacturing in construction
CAD	Computer-aided design
DEM	Discrete element method
FDM	Fused deposition modeling
SLS	Selektives lasersintern
SLA	Stereolithography
DMLS	Direct metal laser sintering
SLM	Selective laser melting
LOM	Laminated object manufacturing
SIS	Selective inhibition sintering
CV	Coefficient of variation
STD	Standard deviation

FG	Functional gradings
NSM	Natur sand mortar
RAM	Mortar with recycled aggregate
SC3DP	Shot-based 3D printing
MMAM	Multi-material additive manufacturing
SPI	Selective Paste Intrusion
DFC	Digital fabrication of concrete

List of symbols

Symbol	Unit	Meaning
μ	[%]	The mean of a group of area fractions
x	[%]	Area fractions
σ	[%]	Standard deviation
P	[%]	Poraver proportion
A	[mm ²]	Poraver area
N	[-]	Poraver particle count

1 Introduction

The construction industry faces significant challenges, including the need to increase efficiency, reduce material consumption, and implement more sustainable construction methods. At the same time, the requirements for the complexity of structures and the customization of construction projects are growing. Against this backdrop, additive manufacturing in construction (AMC), specifically 3D concrete printing (3DCP), is gaining increasing importance. This technology promises to revolutionize the construction of structures by allowing considerable flexibility in design, shortening construction times, and optimizing material use. [Pac-2021]

1.1 Motivation

The construction industry is facing crucial turning points, driven by the quest for efficiency, architectural flexibility, and sustainable building processes. Traditional methods often reach their limits with complex construction projects, efficiency in material use, and acceleration of building processes. In this innovative environment, additive manufacturing (AM), especially 3DCP, is emerging as a key technology to overcome these challenges and lead the construction industry into the digital era. [Bus-2020] Within the additive manufacturing processes in construction, extrusion-based 3D concrete printing technology (E3DCP) plays a powerful role. This technology allows for on-site manufacturing of components, significantly reduces material waste, and realizes unprecedented design freedoms. [Moh-2021] A central challenge is ensuring consistent material homogeneity during the printing process to secure the quality and structural integrity of the printed elements [Wan-2022]. The Gradation-Ready Extrusion System (GRES), equipped with Near-Nozzle Mixing (NNM) process, represents a pioneering innovation in this context. GRES enables the optimization of the material mix directly at the print head just before extrusion. [Add-2024a] This leads to improved material homogeneity and offers the possibility to dynamically adjust material parameters to the specific requirements of each printing process [Chr-2023].

To fully exploit the effectiveness and efficiency of GRES requires a detailed investigation and optimization of the mix quality in the mixing area. This necessitates the development of a specific method for homogeneity analysis. This method should allow for a precise assessment of mix quality, thereby laying the foundation for targeted improvements. This motivation underscores the importance of a systematic classification and optimization of NNM and GRES within the AM processes in

construction. By developing a customized method for homogeneity analysis, the mix quality of GRES can be optimized, significantly contributing to the improvement of quality and reliability of 3DCP and expanding the acceptance and applicability of this innovative technology.

1.2 Objective

One of the goals of this thesis is to develop a systematic classification of the NNM technique (Chapter 3). Through comprehensive literature research, a clear understanding of the current technologies and their applications in AMC will be established. Special attention will be paid to identifying and defining the key characteristics and mechanisms of NNM, to provide a solid foundation for further research and optimization.

Another core objective is to conduct practical experiments with GRES V1.3 (Section 4.1). These experiments aim to investigate the current mixing quality of cement paste and lightweight mortar (LWM) samples produced with GRES V1.3. Following the existing and adjusted recipe (Section 2.3.7) development and successful printing of the mortar samples with GRES V1.3, a careful extraction and processing of the samples will be carried out (Section 4.2). These will then be analyzed using microscopy and image processing to obtain precise cross-sectional images of the mortar structure (Section 4.3). The image processing will be conducted using specially developed Python scripts, enabling efficient and precise evaluation of the mortar's homogeneity. The data obtained will serve for the statistical analysis of material homogeneity (Section 4.4). This analysis includes evaluating the area fraction of Poraver in cement paste and aims to establish a method for assessing mixing quality. The goal is to enable a substantiated evaluation of the current mixing quality of GRES V1.3 through examination of homogeneity, thereby identifying potential optimization points for the system.

In summary, this work focuses on the systematic classification of the NNM process, the execution and analysis of practical experiments with GRES V1.3, and the development of a method for homogeneity analysis. This aims to make a significant contribution to optimizing the mixing quality in E3DCP and lay the groundwork for the future application and further development of the NNM process in construction.

2 State of the Art

AM has emerged as a groundbreaking technology in the construction industry by offering efficient, sustainable, and design-flexible manufacturing methods [Ham-2019]. Section 2.1 is dedicated to the fundamentals of AM, exploring its potential and presenting associated challenges. The focus in Section 2.2 is on 3DCP, a key technology in AMC. One of the main methods, Particle-Bed 3D is discussed. Section 2.3 focuses on E3DCP, another main method of 3DCP and particularly highlights the NNM process (Section 2.3.5). NNM optimizes the printing process by directly mixing the material components at the print head, leading to increased efficiency and better quality [Add-2024a]. The GRES represents a practical implementation of this technology, developed under the Collaborative Research Centre TRR277 Additive Manufacturing in Construction (AMC) and Project A03 [Add-2024b] (Section 2.3.4 and 2.3.6). Furthermore, this chapter examines research on materials and recipes (Section 2.3.7) optimized for E3DCP, especially using the NNM process.

In summary, Chapter 2 provides a comprehensive overview of the current processes and methods of AMC. By conducting a detailed analysis of various manufacturing processes, NNM process, and the development of adapted material recipes, it lays the groundwork for the research and further development of AMC industry.

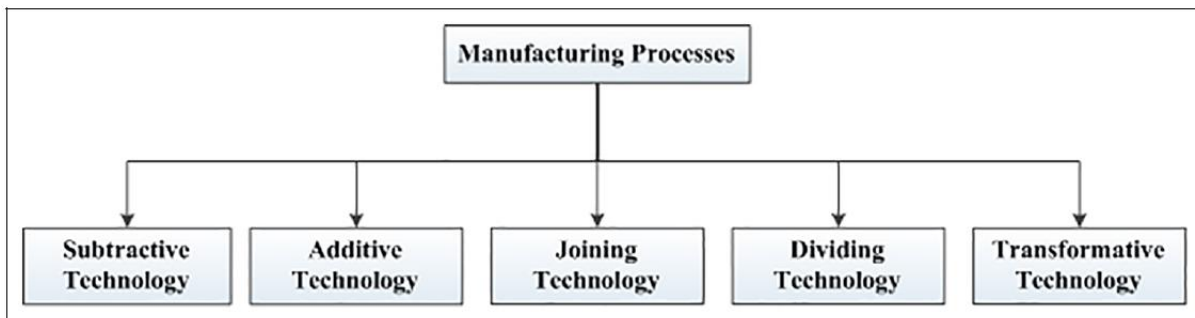
2.1 Additive Manufacturing (AM)

Additive manufacturing (AM), also known as 3D printing, is a groundbreaking manufacturing process. In the international standard ISO/ASTM 52900, AM is defined as a "process of joining materials to make parts from 3D model data, usually layer upon layer [ISO-52900]." This process enables the direct conversion of CAD designs (Computer-Aided Design) into physical objects without the need for traditional molds or tools. It facilitates the efficient production of complex and customized structures with high precision. [Bou-2020]

The core principle of AM is straightforward: an object is formed by gradually adding material, such as plastic, metal, ceramic, or concrete, layer by layer. Each layer represents a thin horizontal cross-section of the final object, and these layers are added successively until the complete object is created. Originating in the 1980s with Chuck Hull's invention of stereolithography, this process allowed for object creation in layers from digital designs, offering unparalleled geometric freedom and adaptability. Over time, AM diversified with the development of sub-processes such as Fused Deposition

Modeling (FDM) and Selective Laser Sintering (SLS), enabling printing with various materials, including metals. As patents expired in the 2000s, innovation in AM surged, making it more accessible. Initiatives like RepRap promoted open-source 3D printing technologies, driving the maker movement forward. In recent years, 3D printing has gained widespread acceptance across industries such as aerospace, automotive, construction, and medicine, used for tailored solutions and waste reduction. Today, AM stands on the brink of new breakthroughs, including bioprinting, which promises to advance design, manufacturing, and sustainability efforts even further. [Pei-2023]

Figure 2-1: Classification of manufacturing processes [Abd-2019]



AM falls into one of the five categories of manufacturing processes: subtractive, additive, joining, dividing, and transformative () [Abd-2019]. It can be categorized based on the materials used, employing fusion, binding, or solidification methods, which results in a diverse array of technologies and applications (Figure 2-2) [Abd-2019]. Plastics are extensively utilized due to their versatility and ease of processing, with techniques like Fused Deposition Modeling (FDM) and Stereolithography (SLA) commonly employed for prototypes and low to medium stress end products. Metals, processed through methods such as Direct Metal Laser Sintering (DMLS) and Selective Laser Melting (SLM), play a vital role in aerospace, automotive, and medical technology by enabling the production of robust parts with intricate geometries. Ceramics find application in fields like dentistry and biomedicine, where precision and material durability are essential. Concrete is transforming construction by enabling the printing of large structures directly on-site, saving time and offering design flexibility. Furthermore, emerging developments such as bioprinting and the use of composite materials are driving research toward customized implants and multifunctional parts. Structuring AM according to materials underscores the adaptive capabilities of these technologies, ranging from the micro-level of biological structures to large-scale construction, reflecting an ecosystem of innovations tailored to the specific strengths of each material. [Bou-2020]

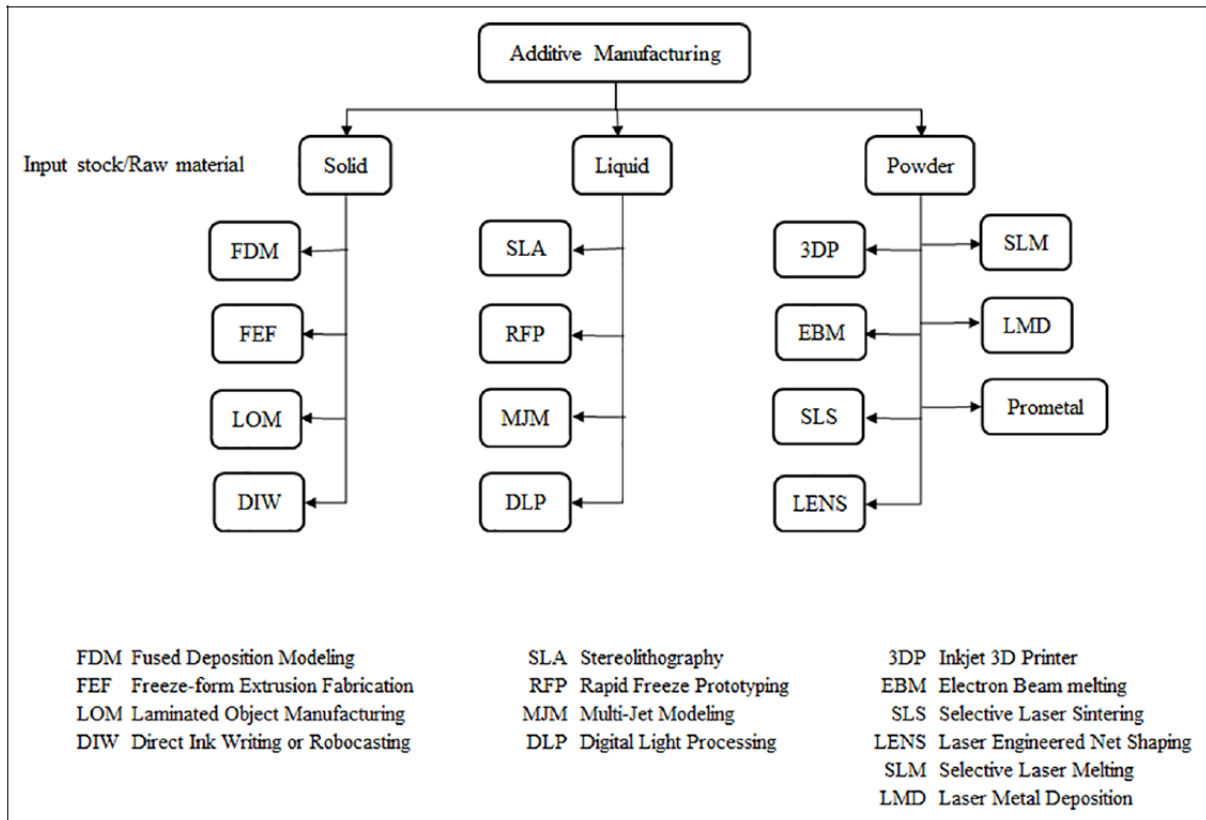


Figure 2-2: Classification of AM processes depending on the state of raw material [Abd-2019]

In addition to materials, AM can also be classified based on the respective manufacturing process into seven categories: material extrusion, material jetting, binder jetting, powder bed fusion, directed energy deposition, vat photopolymerization, and sheet lamination [ISO-52900]. Material Extrusion employs a nozzle to extrude materials like plastic, known as FDM. Vat Photopolymerization cures liquid photopolymers through UV light, with Stereolithography (SLA) being a prominent example. Powder Bed Fusion fuses powder materials layer by layer using a laser or electron beam, including techniques like SLS and DMLS. Material Jetting sprays liquid material that is subsequently cured, enabled by PolyJet. Binder Jetting binds powder particles with a binder to form diverse materials. Sheet Lamination combines layers of paper or metal, as applied in Laminated Object Manufacturing (LOM). Directed Energy Deposition directs an energy beam onto material, which is melted at the point of contact, often used for metal repairs. [Pao-2019]

2.2 3D Concrete Printing (3DCP)

Aggregate-based materials such as concrete are prevalent in the field of additive construction [Pao-2019]. The term 3D concrete printing (3DCP) denotes the application of large-scale AM technologies to concrete and concrete-like materials in construction, constituting a specialized form of 3D printing [Bus-2020]. This technology transcends traditional boundaries, offering new avenues for design freedom, efficiency, sustainability, and customization in construction projects [Pao-2019]. The origin of 3DCP can be traced back to the broader development of AM technologies in the late 20th century. As AM techniques advanced, particularly in the realm of material extrusion, researchers began exploring the possibility of applying similar principles to concrete construction. One of the early milestones in the development of 3DCP was the creation of Contour Crafting technology by Dr. Behrokh Khoshnevis at the University of Southern California (USC) in the early 2000s. Contour Crafting aimed to automate building construction using large-scale 3D printers capable of extruding concrete in layers to construct structures incrementally. This breakthrough paved the way for further research and development in 3DCP, leading to the exploration of various printing techniques, concrete formulations, and construction applications [Bus-2020]. Today, 3DCP is recognized as a promising technology with the potential to revolutionize the construction industry by enabling rapid, cost-effective, and sustainable fabrication of complex architectural designs and infrastructure [Pao-2019].

In terms of efficiency and speed, 3DCP offers significant advantages. By manufacturing components directly on-site or in a factory followed by assembly at the destination, construction times can be significantly reduced. Loughborough University constructed a curved bench measuring $2 \times 0.9 \times 0.8 \text{m}^3$ based on its 3DCP concept, with the printing process taking approximately 42 hours (Figure 2-3) [Lim-2012]. Similarly, XtreeE printed a complex-shaped wall element measuring $1.36 \times 1.50 \times 0.17 \text{m}^3$ using a 6-axis robot arm, with a production time of about 12 hours [Gos-2016]. WinSun printed the components of a single-floored office building covering almost 250m^2 for the Dubai Future Foundation (see Figure 2-3). The printing process, similar to Contour Crafting, spanned 17 days, after which the parts were transported to Dubai and assembled in 2 days. [Del-2018] In the Netherlands, Eindhoven University of Technology constructed a bicycle bridge with a span of 6.5m and a width of 3.5m using 3DCP. All elements were printed within 48 hours. [Sal-2018] This method also reduces the need for extensive formwork and manual labor, resulting in cost savings. Additionally, 3DCP offers sustainability benefits by minimizing material consumption and waste, thus reducing the CO₂ footprint of construction projects and promoting environmentally friendly construction processes. The customization and adaptability of building elements through 3D printing are also noteworthy, allowing each element to be designed according to

specific requirements and local conditions, thereby elevating the personalization of buildings to a new level. [Sid-2020]

Figure 2-3: *Left: Curved bench constructed by Loughborough University [Lou-2023]. Right: Office building constructed by WinSun [Mic-2016].*

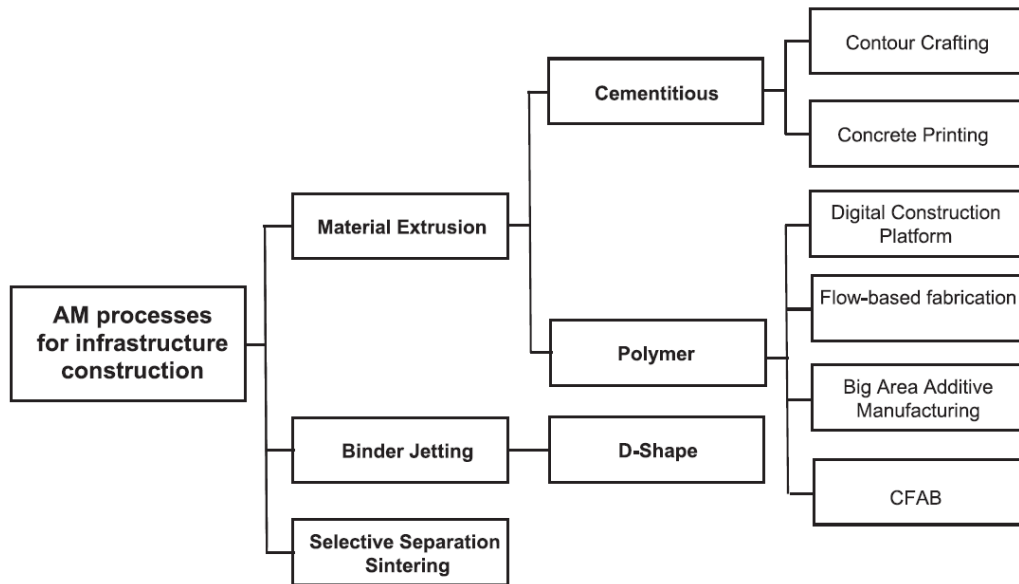


Despite these potentials, challenges such as ensuring structural integrity, scaling printing processes for large projects, and developing industry standards remain. Ongoing research and innovation in material mixes, printing techniques, and post-processing methods are crucial to overcome these challenges and realize the widespread application of concrete in additive manufacturing in construction. [Sch-2018]

In the realm of 3DCP, the development of various processes has contributed to fully exploiting and expanding the potential of concrete printing in construction (Figure 2-4). These technologies vary in their processing methods and offer unique benefits for specific applications. Primarily, concrete printing utilizes material extrusion and particle-bed processes, although alternative generative methods like Smart Dynamic Casting have also been studied [Pao-2019]. Extrusion-based 3D concrete printing (E3DCP), which presses concrete through a nozzle and applies it in precise layers, allows for the construction of complex structures with high flexibility. The use of a robotic arm can further increase geometric freedom. [Alt-2022] Particle-Bed 3D Printing (Section 2.2.1), works with a powder bed onto which a binder is sprayed to connect the particles and form the object. This method is particularly suited for detailed architectural elements. [Low-2018] In Shotcrete-Based 3D Printing (SC3DP) (Section 2.3.2), concrete is sprayed under pressure onto a surface, enabling rapid construction of structures and is mainly used for free-formed structures [Hei-2022]. Another method, Slip Forming 3D Printing, uses a movable form to continuously shape the concrete into the desired form, ideal for columns and vertical elements [Ruf-2022]. Contour Crafting, an automated construction technique, lays down concrete along predefined paths, enabling rapid erection of building walls. Selective Inhibition Sintering (SIS) for concrete and Binder Jetting with concrete are more innovative approaches that further explore the field by pioneering new ways of material hardening and binding [Bou-2020]. This variety of methods in additive manufacturing with concrete opens up unprecedented possibilities in construction, from realizing sophisticated designs to optimizing construction times

and material consumption, and highlights the transformative potential of the technology for the industry.

Figure 2-4: Process classification [Bus-2020]



2.2.1 Particle-Bed 3D Printing

Particle-bed 3D printing stands as an AM process, utilized to craft intricate free-form structures directly from a 3D computer model. Similar to other AM processes, it constructs objects layer by layer. The process initiates with the application of a layer of dry particles, followed by the selective deposition of a fluid phase to bind the particles, typically executed through a print head or nozzle. Subsequently, non-bonded particles undergo removal in a depowdering process. Post-processing techniques such as infiltration or heat treatment can then be applied to bolster the strength and durability of the final product. In the realm of producing concrete components, three primary strategies are employed (Figure 2-1): Selective Cement Activation (SCA), involving the localized activation of cement; Selective Paste Intrusion (SPI), entailing the coating of aggregate particles with a cement paste; and Binder Jetting, facilitating the printing of permanent formwork that becomes composite with poured concrete. [Low-2018]

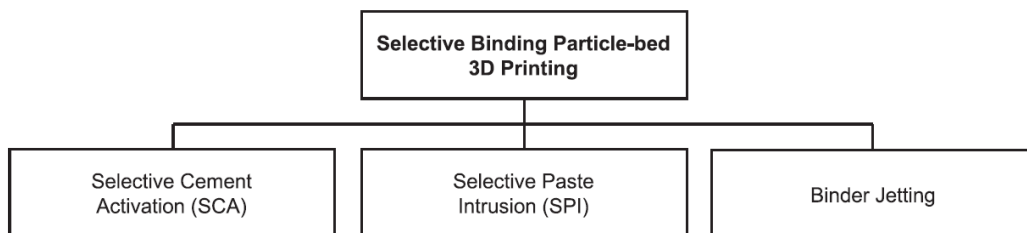


Figure 2-5: Process classification of particle-bed methods [Bus-2020]

These processes are distinguished by the materials utilized (Figure 2-6). In SCA, cement is locally activated by water spray or jetting, forming a cement paste matrix around aggregate particles. In SPI, aggregate particles are coated with a binder paste comprising cement, water, and admixtures to produce components with sufficient strength. In Binder Jetting, a liquid binder, typically resin, is applied to a particle bed, reacting with a hardener component within the bed. [Low-2018]

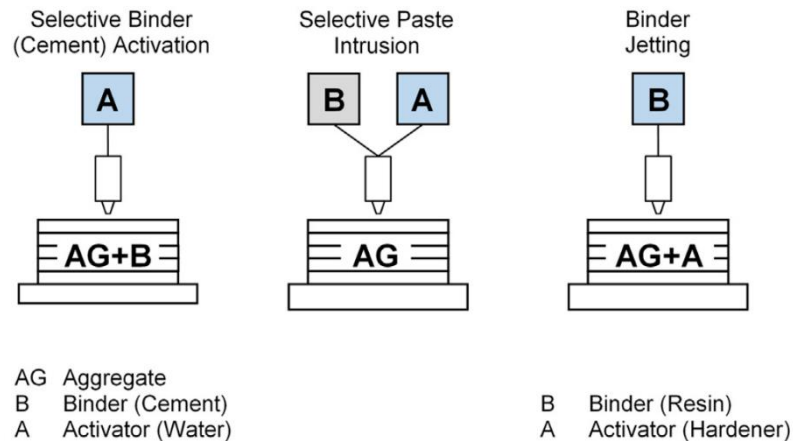


Figure 2-6: Schematic figure of particle-bed 3D printing techniques in construction [Low-2018]

Particle-bed 3D printing offers several advantages over other construction AM processes. It enables the creation of structures with complex geometries, including inclined structures, arches, and cantilevers, with high resolution and production speed. However, the size of components is limited by printing space, although large-scale printers are emerging. Despite challenges such as variability in mechanical properties and post-processing needs, particle-bed 3D printing presents innovative possibilities for the construction sector, expanding design limits and enabling the production of highly precise, complex components. [Low-2018]

2.3 Extrusion-Based 3D Concrete Printing (E3DCP)

Extrusion-based 3D concrete printing (E3DCP) is a subset of 3DCP that has gained recognition from both academia and industry as a promising method for future concrete construction projects. Its potential has been validated through various industrial endeavors by construction firms such as XTree, COBOD, WASP, WinSun, Sika, and others. Notably, E3DCP excludes injection-based 3D concrete printing, smart dynamic casting, and shotcrete-based 3D concrete printing. [Che-2023] Among the array of techniques, E3DCP stands out as a viable solution for large-scale applications, particularly in concrete and mortar printing. It serves as a pivotal technology within the realm of 3DCP, facilitating the direct translation of digital designs into tangible concrete structures. Utilizing computer-controlled extrusion processes, E3DCP involves pressing a

concrete mix or similar material through a specialized nozzle, meticulously layering it to construct the desired object incrementally. [Moh-2021]

In E3DCP, concrete is extruded continuously or discontinuously from the nozzle as it follows predetermined paths. This motion is guided by a robotic arm or another automated system programmed based on digital CAD models, enabling the creation of intricate shapes and structures that were once challenging to achieve with conventional construction methods. This method boasts several notable advantages, making it a groundbreaking technology in modern construction. Firstly, E3DCP offers unparalleled design freedom, empowering architects and engineers to conceive innovative structures previously deemed unattainable due to technical constraints. Additionally, its efficiency significantly reduces construction time by minimizing or eliminating the need for formwork and enabling on-site or prefabricated component production. Moreover, E3DCP promotes sustainability by optimizing concrete material usage, thereby reducing waste and environmental impact. The precise deposition of concrete only where needed further enhances resource efficiency. Ultimately, these efficiency gains translate into substantial cost savings, making E3DCP an attractive option for forward-thinking construction projects. However, several challenges must be addressed to fully harness the potential of E3DCP. Material development remains a key concern, necessitating the formulation of concrete mixes that exhibit optimal flow properties and mechanical strength post-curing. Ensuring the structural integrity and durability of printed structures also poses a significant challenge, requiring rigorous testing and meticulous planning. [Mec-2020]

To comprehensively classify E3DCP, a classification framework has been devised for feasible digital fabrication of concrete (DFC) technologies (Figure 2-7). This framework delineates a multifaceted process chain wherein a primary process (such as shaping or assembly) and a suite of sub-processes (integral steps occurring during the execution of the primary process) are identified. Within E3DCP, the primary process is shaping, encompassing extrusion and deposition processes. [Che-2023]

Despite these obstacles, E3DCP represents a transformative process in the construction industry, offering unprecedented capabilities in creating building structures and elements through layer-by-layer concrete deposition. With ongoing advancements in material science and printing processes, coupled with the design and adaptation of printing systems, E3DCP continues to evolve, promising to revolutionize construction processes and redefine architectural possibilities.

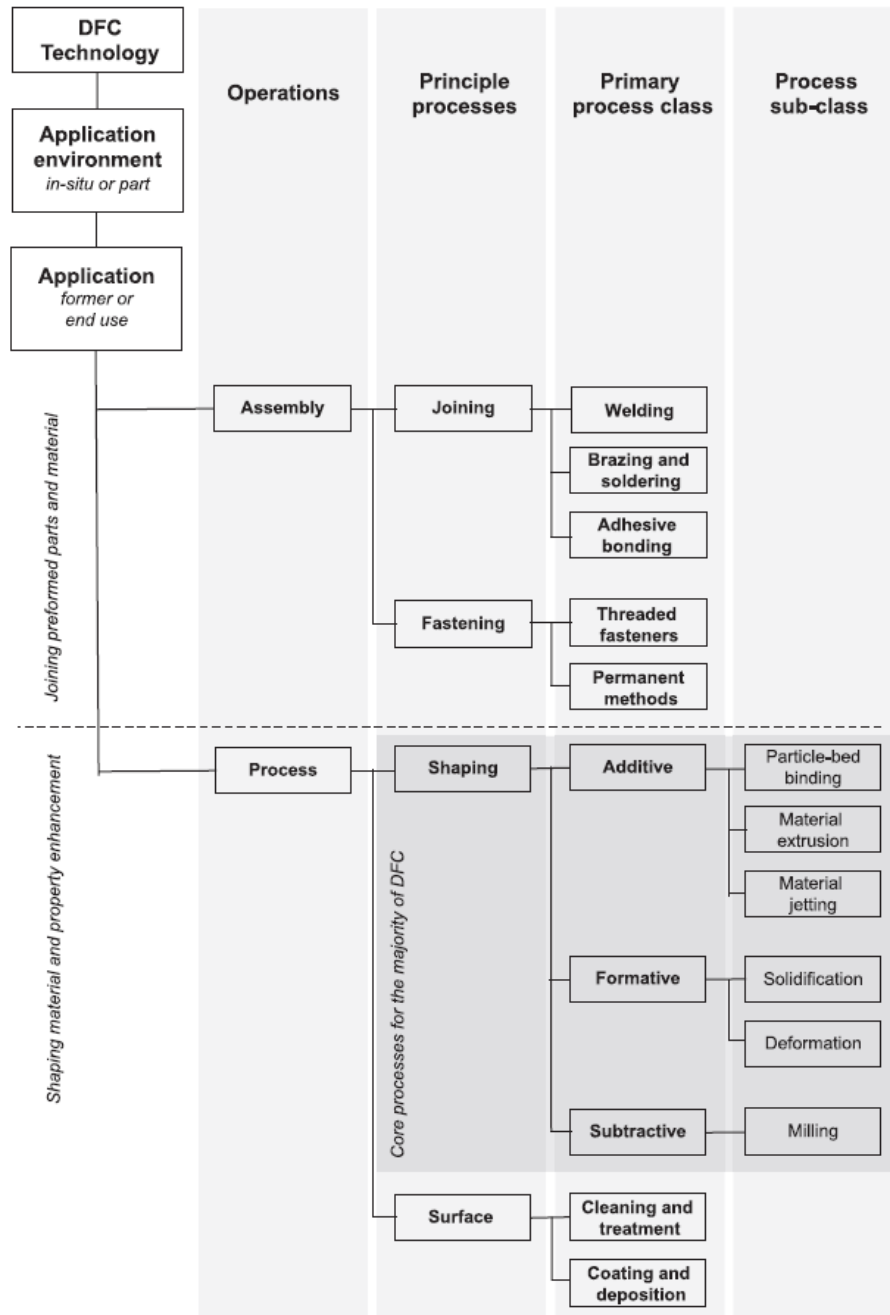


Figure 2-7: The RILEM process classification framework for DFC technologies [Bus-2020]

2.3.1 Digital concrete processing

Digital concrete processing encompasses a series of steps aimed at producing self-supported 3D printed material. These steps include mix proportioning, primary (1st) mixing, storage, transport/material delivery, secondary (2nd) mixing, application, finishing, and curing (strength buildup) (Figure 2-8). [Wan-2022]

Mix proportioning involves weighing defined quantities of dry materials, water, chemical admixtures, and other components, typically done through batch processing or pre-dosing into drymix batches. Primary mixing, the next step, entails adding water to the

dry materials and dispersing them homogeneously using mechanical energy to initiate contact between water and the materials. Storage, commonly preceding other process parts, involves storing the material before feeding it into a pumping system, often via batches or hopper systems. Transport/material delivery consists of delivering the material to the printhead, usually achieved through pumping with progressive cavity pumps or positive displacement piston pumps. Secondary mixing involves injecting additives at the printhead for stiffening control or other purposes, typically performed by active mixers or static mixers. This step is crucial for enhancing buildability and facilitating processing in the printhead. Application is the extrusion of material from the printhead, with specific requirements related to filament shape and viscosity to prevent cracking and ensure proper flow. Some technologies include a finishing step where the material is shaped either concurrently with extrusion or afterward. Finally, curing, essential for strength buildup, involves allowing the concrete to develop strength to support further layers. This step may also involve moisture management to prevent cold joints and ensure proper curing conditions for optimal material properties. [Wan-2022]

1K and 2K systems refer to different types of digital concrete processing systems based on the number of components involved in the mixing process. In a 1 component systems (1K) system, the concrete mixture is pre-prepared with all necessary components, such as aggregates, cement, water, and admixtures, combined into a single mixture. This single mixture is then transported and applied directly during the printing process. On the other hand, a 2 component (2K) system involves the use of separate components that are mixed together at the point of application. Typically, one component contains the dry materials, such as aggregates and cement, while the other component contains the liquid components, such as water and admixtures. These two components are mixed together either at the nozzle or just before extrusion, allowing for greater control over the properties of the concrete mixture and the printing process. [Wan-2022]

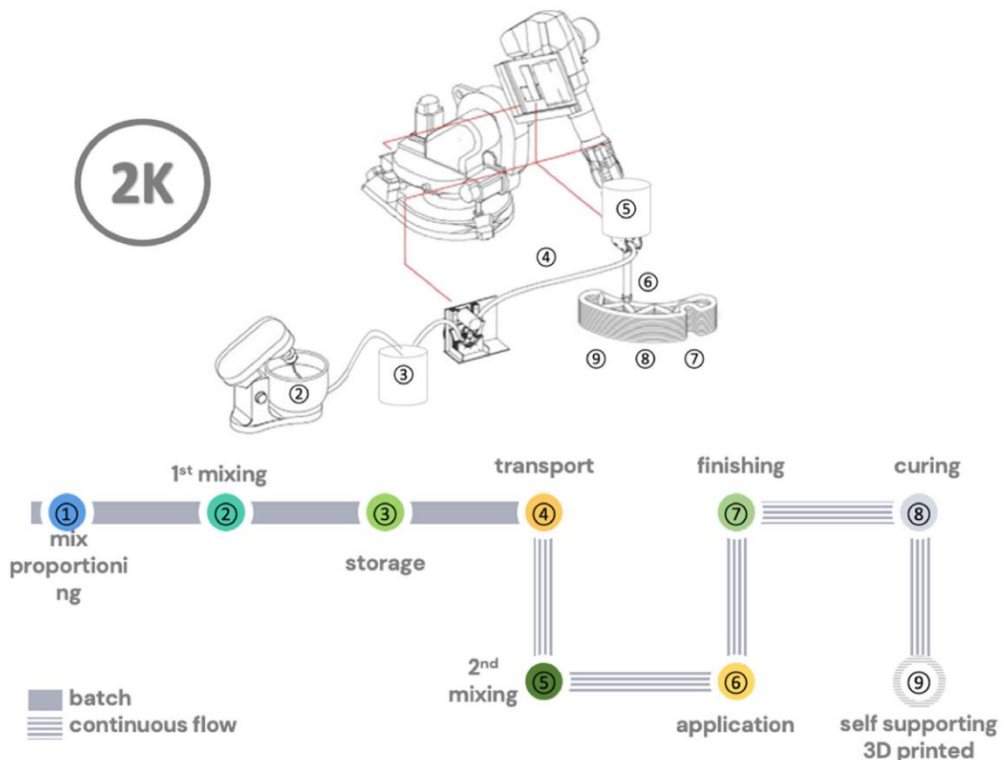
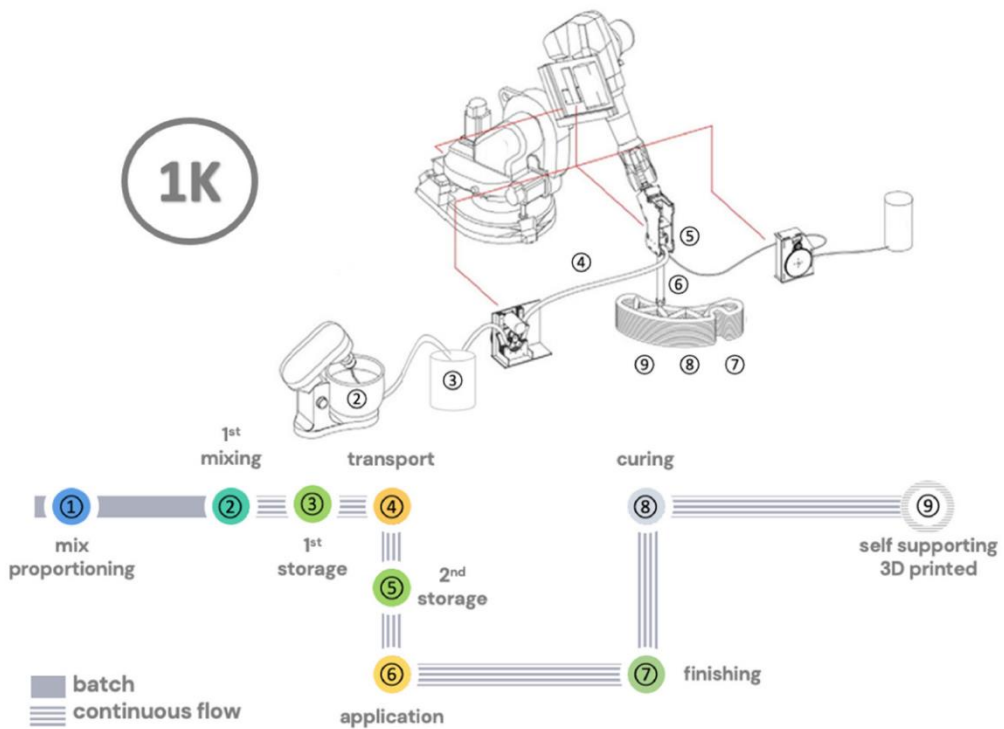


Figure 2-8: Illustration of various processing steps in concrete extrusion 3D printing processes. 1K do not include the secondary mixing step of an accelerator just before extrusion, as in the 2K systems. [Wan-2022]

2.3.2 Shotcrete-based 3D printing (SC3DP)

Shotcrete-based 3D printing (SC3DP) has emerged as an alternative concrete AM process to address the limitations of extrusion-based printing, such as weak interlayer bond and challenges in building overhangs and vertical elements. In SC3DP, printing layers are formed through a shotcreting process rather than extrusion. By utilizing substrate, formwork, or reinforcement meshes, SC3DP enables the construction of vertical and overhanging elements with ease. Researchers have also achieved free-formed SC3DP by employing a printing path similar to traditional extrusion-based printing but with enhanced interlayer bond (Figure 2-9). [Hei-2022]



Figure 2-9: *Left: SC3DP with substrate/reinforcement [Hei-2022]; Right: Free-formed SC3DP [Lu-2020]*

Traditionally, shotcrete can be applied in two ways: the dry-mix process and the wet-mix process, with the main difference being the timing of water addition to the mixture. The wet-mix shotcrete method is generally preferred by engineers due to its reduced dust and rebound production. While shotcrete traditionally requires manual operation, recent advancements in robotics have enabled automated shotcrete processes, naturally leading to the development of SC3DP. In SC3DP, concrete layers are deposited through a shotcrete process onto existing substrates or previously printed layers. [Hei-2022]

One of the key advantages of SC3DP is its ability to efficiently construct free-formed and geometrically demanding structures without relying on traditional formwork methods. This not only accelerates the construction process but also provides flexibility in processing concrete mixtures with diverse properties, ranging from fast-drying to high-structural-integrity mixes. SC3DP allows engineers to construct overhangs and vertical surfaces easily, offering a high placing rate and efficient material compaction. Elements fabricated using SC3DP demonstrate intense interlocking between printed layers, resulting in high interlayer bond and mechanical performance. Despite its advantages, SC3DP users encounter challenges such as ensuring uniform surface quality and guaranteeing the structural integrity of printed objects. Challenges associated with shotcrete construction include material loss due to rebound and excessive dust

on the construction site, which can impact material properties and placement. Additionally, achieving high geometry precision in SC3DP is more complex than in extrusion-based 3D printing due to the control of various parameters. [Hei-2022]

Overall, SC3DP combines architectural freedom with construction efficiency, exemplifying the integration of robotics and digital manufacturing in construction to reduce costs, accelerate the building process, and unlock new design possibilities.

2.3.3 Multi-Material Additive Manufacturing (MMAM)

Multi-Material Additive Manufacturing (MMAM) is a burgeoning approach in the realms of architecture and construction, extending the capabilities of Additive Manufacturing. MMAM involves the integration of different materials or material properties within a single additive process to fabricate objects composed of multiple materials. Unlike conventional construction methods, which rely on assembling single materials or elements, MMAM enables the creation of objects with diverse material properties without the need for subsequent assembly. This shift can streamline manufacturing and construction processes by reducing the number of production steps required and addressing challenges associated with connecting individual materials or elements. Additionally, transitioning from single-material to multi-material processes not only enhances the manufacturing and construction process itself but also unlocks extensive design possibilities. Architect Tom Wiscombe emphasizes this potential, stating that MMAM allows for customization of structural rigidity and material responses to various criteria simultaneously, expanding design horizons. This evolution towards MMAM also fosters sustainability by optimizing material usage and tailoring individual components to environmental requirements. [Paj-2022]

MMAM encompasses various processes categorized based on how multiple materials are integrated. These processes can involve discrete placement of different materials next to each other, control of porosity, or blending of materials. Most AM processes inherently support the integration of multiple materials, achieved by including more than one material or modifying material properties through processing parameters. Compared to single-material processes, MMAM has the potential to fundamentally transform product and structure creation by enabling seamless integration of different materials within a single manufacturing process. While AM processes in architecture and construction are primarily single-material, initial forays into MMAM are underway, with ongoing exploration of potential advantages and drawbacks. [Paj-2022]

The categorization of MMAM within Material Extrusion highlights two main approaches: processes that simultaneously process and deposit multiple materials and processes

that blend different materials before deposition (Figure 2-10). Within these categories, further subdivisions exist based on specific characteristics. Processes involving parallel extrusion are divided into Direct Ink Writing (DIW) and Concrete Printing or Fused Deposition Modeling (FDM) processes. On the other hand, processes blending different materials can be categorized into those where each mixture represents specific material properties and can function independently, and those with a primary material mix supplemented by selectively added additives or fillers. [Paj-2022]

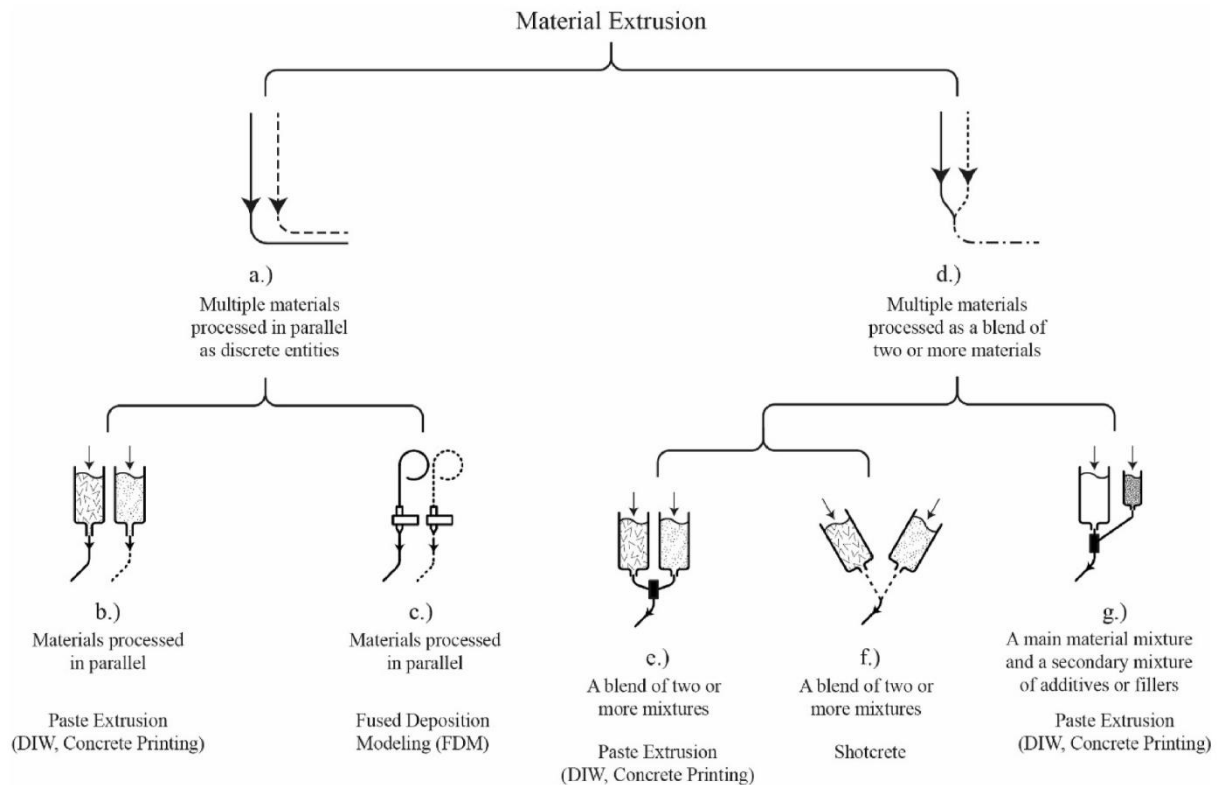


Figure 2-10: Categorization tree for MMAM Processes in Architecture and Construction [Paj-2022]

In construction-scale AM, material extrusion processes are prevalent, with concrete being a commonly used material. Other materials, such as polymers, are also utilized for specialized applications like creating formwork with insulation properties. MMAM approaches within material extrusion involve either processing multiple materials simultaneously or blending materials before extrusion. Systems with parallel extrusion units facilitate discrete placement of multiple materials, while processes blending materials before extrusion allow for seamless transitions between different material compositions. Despite the advantages of MMAM, challenges such as monitoring material gradients and managing mixing complexities need to be addressed for its widespread adoption and integration into construction practices. [Paj-2022]

2.3.4 Collaborative Research Centre TRR277 AMC and Project A03

The Collaborative Research Center TRR 277 Additive Manufacturing in Construction (AMC), an initiative of the Technical University of Braunschweig and the Technical University of Munich, has been researching pioneering AMC technologies since 2020. Researchers from the fields of architecture, civil engineering, and mechanical engineering at the universities collaborate in an interdisciplinary environment to explore the fundamentals of AMC technology. This technology is considered a key to advancing digitization, resource efficiency, and productivity in the architecture, engineering, and construction sectors. The focus is on investigating new technologies in various material and process combinations, employing an integrative research approach that considers structural design, material technology, and manufacturing processes as a unified entity. [Add-2024b]

Project A03, with Maximilian Dahlenburg and Christian Maximilian Hechtel as contributors, and Maximilian Dahlenburg as the research focus of the TRR 277 AMC, is dedicated to the development and exploration of NNM for E3DCP. This innovative process enables a revolutionary approach in construction by mixing material components directly at the print head, significantly reducing the transport distance through hoses and decreasing the associated required pump pressure. Over the past four years, a functional NNM system, called the Gradation-Ready Extrusion System (GRES), has been developed. This system has demonstrated the ability to print a variety of mortar compositions, from natural sand mortars to lightweight mortars. This concept enables new design approaches, more efficient resource utilization, and tailored product characteristics, raising numerous interdisciplinary research questions such as material compatibility, properties of transition zones, design approaches, and overall performance. In addition to optimizing the system and developing mixtures, the project focuses on creating detailed application concepts (graded element designs). These updates to the system, an expanded range of material compositions, and application concepts are applied to advance systematic knowledge of NNM-3DCP-based functional grading. This involves establishing relationships between material properties (in the fresh and hardened states) and NNM process parameters, especially at the transition between different material compositions, as well as understanding the effects of graded materials on printed objects. [Add-2024a]

Overall, project A03 within the TRR 277 AMC promises, through its interdisciplinary research, to not only expand the technical feasibility and academic understanding of functionally graded 3DCP but also to chart new directions for the construction of the future by merging ecology and economy through innovative AM techniques in construction. [Add-2024a]

2.3.5 Near-Nozzle-Mixing (NNM)

Near-Nozzle Mixing (NNM) is an innovative approach in the field of 3DCP, aiming to optimize the composition of concrete materials just before their extrusion through the nozzle. This process strives to ensure consistent and uniform material consistency, which minimizes interruptions in the printing process and enhances the final quality of the printed structures. [Add-2024a] NNM enables dynamic adjustment of the mix composition in real-time, which particularly facilitates the application of various concrete formulations for specific requirements or components. This process enhances the flexibility and adaptability of 3DCP by allowing targeted and efficient processing of materials with diverse properties, such as different strengths, densities, or thermal insulation characteristics. [Chr-2023]

At the core of this technique is the idea of mixing the components of concrete (cement, water, and possibly additives) only immediately before extrusion through the nozzle. This method differs fundamentally from traditional E3DCP processes that work with a pre-prepared and mixed concrete mass. The main feature of NNM is the positioning of the mixing process directly at or near the print head. By combining the dry and liquid components of the concrete shortly before deposition, NNM allows for high flexibility in adjusting the mix during the printing process. This can be particularly advantageous to respond to rapid changes in printing conditions or to tailor specific properties of the concrete for different parts of the printed object. [Add-2024a]

In comparison to traditional extrusion methods, the NNM stands out for two significant advantages: Firstly, it eliminates the need for mortar conveying, simplifying the overall process and reducing the requirements for material workability. Secondly, the NNM technique provides the opportunity to integrate multifunctional properties into printed objects by selectively implementing material specifications at specific locations. This means that even stiff mortars, which are typically considered non-pumpable, can be efficiently processed using NNM technology. This opens up new avenues for the future of mortar and concrete printing, especially as demand for efficient, sustainable, and adaptable construction methods increases. NNM technology lays the foundation for further exploration in the realm of multi-material printing by allowing for the adaptation of material composition during the printing process. This enables the development of structures with functionally graded materials or embedded functionalities, highlighting the versatility and adaptability of the NNM process and positioning it as a promising technology for AM in the construction industry. [Chr-2023] Introducing NNM into E3DCP brings significant advantages, but also presents considerable challenges. One of the biggest obstacles lies in the technical complexity associated with reliably implementing an NNM system. For effective application, it is necessary to develop advanced technical solutions that ensure a uniform mixture of concrete components and a

constant supply of material. This requires not only precise control of the mixing process directly before or within the print head but also careful coordination of components and the extrusion process. [Add-2024a] Additionally, quality control plays a crucial role in the success of NNM. The properties of the finished concrete product (strength, density, and other important characteristics) are significantly influenced by the accuracy of the mixing process and the uniformity of the concrete mixture. To ensure high-quality printed structures, continuous monitoring of the mixing process and fine adjustment of the material composition are therefore required. These requirements underscore the importance of precise control systems and careful process management to fully leverage the benefits of NNM while successfully addressing the challenges related to technical implementation and quality control. [Chr-2023]

2.3.6 Gradation-Ready Extrusion System (GRES)

The Gradation-Ready Extrusion System (GRES) is a functional NNM system developed within the scope of project A03. This system minimizes the transport distance of materials through hoses, thereby significantly reducing the required pump pressure. GRES enables the processing of specially tailored, sustainable mortars and concretes that would not be printable with conventional 3DCP systems. [Tan-2022]

In its current form, GRES V1.3 comprises several essential components (Figure 2-11). These include a dry hopper for aggregates, a controllable motor facilitating aggregate feeding and mixing, and a mixing area equipped with a mixing shaft housed within a sufficiently long mixing chamber. To prevent the formation of dead zones where material could accumulate and harden, particular attention is paid to the design of the mixing area. Additionally, the compression area features active stirring paddles and a cylindrical mixing chamber, which contribute to an efficient mixing process and facilitate material transportation to the extrusion chamber. [Add-2024a] The workflow of GRES V1.3 begins with the conveyance of aggregates from the hopper to the mixing area via a screw conveyor. In the mixing area, the aggregates are homogenized with the cement paste, which is prepared in the mixer and then circulated in a barrel. Subsequently, the mixture is pumped through a squeezing pump into the mixing chamber. Upon entering the compression area, the material is kept in motion by the extrusion shaft until it is finally extruded.

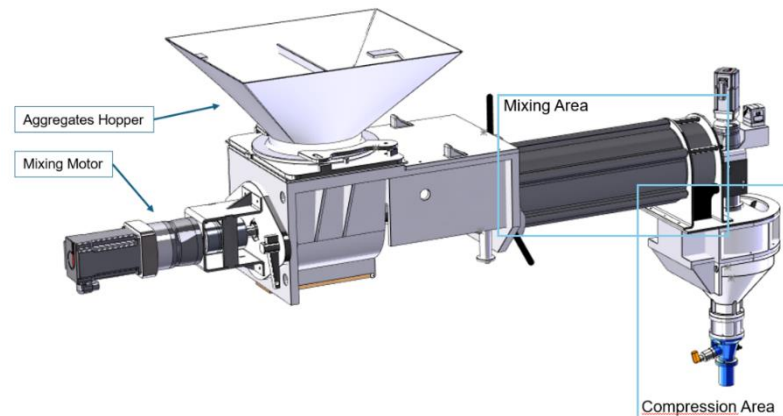


Figure 2-11: CAD Modell of GRES V1.3

GRES V1.3 demonstrates impressive results; however, it has some limitations, such as the capacity to hold different materials simultaneously and monitoring of material composition versions. These limitations are intended to be addressed through the development of an updated version of GRES, which includes multiple reservoirs for different aggregates and fibers, as well as the ability to adjust the cement paste. [Add-2024a]

2.3.7 Material and Recipe

With the progressive demonstration of its capabilities, the NNM process has increasingly attracted interest in research to explore its potential for diverse applications. Particularly, the possibility of multi-material printing using NNM process is the focus of current investigations. In this context, three mortar variants have already been thoroughly analyzed: natural sand mortar (NSM), mortar with recycled aggregate (RAM), and lightweight mortar (LWM) [Chr-2023]. These variants represent a spectrum of materials that highlight the versatility and adaptability of the NNM process, showcasing its potential for future applications in E3DCP and mortar.

The Lightweight Mortar (LWM) is developed using expanded glass aggregates from PORAVER[®], consisting of a gradation that includes particle sizes of 0.1-0.3 mm, 0.25-0.5 mm, 0.5-1.0 mm, and 1.0-2.0 mm [Chr-2023]. This variant proves to be particularly relevant for the present study. Poraver, made entirely of recycled glass and purely mineral, is characterized by its pronounced environmental friendliness. It not only provides thermal insulation but also acts as a sound absorber, remains permanently dimensionally stable, and exhibits resistance to temperature fluctuations, moisture, and chemical substances [Por-2024]. The composition of the LWM includes the cement paste and the aggregate poraver. Achieving a reproducible, printable, and structurally workable mortar mixture relies significantly on the precise formulation of the cement

paste and mortar. An appropriate formulation has already been researched and is continuously undergoing optimization. The cement paste in the formulation consists of conventional Portland cement CEM I 52.5 R, silica fume, limestone powder, and tap water, enriched with a superplasticizer based on Polycarboxylateether (PCE) to ensure the necessary workability. The exact proportions of the paste, as well as the water-cement ratio (w/c) of 0.58 and a density of 1.87 kg/dm³, are listed in Table 2-1 [Chr-2023].

Table 2-1: Composition of the cement paste [Chr-2023]

Materials	Percentage (M. %)
CEM I 52.5 R	54.5
Water	31.0
Silica fume	5.0
Limestone powder	10.0
Superplasticizer	0.5

All mortars used the same cement paste as the binder, supplemented with different types of aggregates. The volume ratio of aggregates to paste was maintained at 3:2 for all mortars. Table 2-2 shows the maximum particle sizes and bulk densities of the poraver as aggregate. [Chr-2023]

Table 2-2: Characteristics of the LWM composition [Chr-2023]

Mortar	Max. Grain Size [mm]	Grain Density [kg/dm ³]	Calculated Mortar Density [kg/dm ³]
LWM	2	0.40	1.11

The analysis of LWM properties based on the depicted formulations in the fresh and hardened states, as shown in Table 2 3, underscores the consistency in the performance of the printed LWM.

Table 2-3: Material performance for LWM in the fresh and hardened state; measured mean mortar property with the standard deviation (STD) and related coefficient of variation (CV). [Chr-2023]

Fresh parameters	LWM
Slump Flow Paste	374 ± 1.41 (0.38%)
Slump Flow Mortar	157.5 ± 8.02 (5.09%)
Yield Stress	377 ± 5.49 (1.46%)
Density (Fresh)	1.17 ± 0.01 (1.21%)
w/c Ratio	0.59 ± 0 (0.46%)

Air Void Content	14.5 ± 0.71 (4.88%)
Hardened parameters	LWM
Compressive Strength	21.8 ± 2.52 (11.54%)
Flexural Strength	1.3 ± 0.47 (36.34%)
Density (Hardened)	1.13 ± 0.03 (2.83%)
Thermal Conductivity	0.38 ± 0.01 (2.64%)

In particular, the LWM exhibits lower density and thermal conductivity, good flow limit, and high workability. Furthermore, it demonstrates stable load-bearing capacity with minimal fluctuations during the printing session. With sufficient compressive strength of 21.8 MPa, a density of 1.13 kg/dm³, and a low thermal conductivity of 0.38 W/mK, certifying insulating properties, the LWM demonstrates excellent material qualities. This confirms that LWM, manufactured according to the specified formulations and extruded using NNM technology, offers outstanding material properties for the 3D construction sector.

To control the quality of cement paste and mortar, spread test should be additionally integrated. The spread test for cement paste is a straightforward yet valuable method for assessing its flowability, and consequently, indirectly determining its consistency and workability. This test holds particular significance during the mortar preparation stage for 3D printing, as it allows for the evaluation of material homogeneity and printing properties. The procedure for conducting the spread test aligns with DIN EN 1015-3: "Test methods for mortar for masonry - Part 3: Determination of consistence of fresh mortar (by flow table)."

2.4 Homogeneity Analysis

This Chapter provides a comprehensive overview of the methods employed to conduct this study, with a focus on the homogeneity analysis of mortar mixtures. It begins by addressing the homogeneity analysis in detail, starting with a clear definition of homogeneity (Section 2.4.1), followed by the introduction of various methods for homogeneity analysis (Section 2.4.2) and a discussion of statistical techniques for assessing homogeneity (Section 2.4.3).

A homogeneity analysis is a crucial part of many scientific and engineering disciplines, focusing on determining the uniformity of a substance, material, or process [Yuc-2019]. In the context of E3DCP, especially with techniques like NNM, homogeneity analysis plays a vital role in ensuring that the concrete mixture maintains consistent properties throughout. This is critical for the structural integrity and quality of the printed objects.

[Chr-2023] Homogeneity analysis typically involves tests and procedures to quantitatively assess the distribution of components within a sample [Yuc-2019]. For concrete, these components might include cement, water, aggregates, and additives. A uniform distribution of these components is crucial for the mechanical properties of cured concrete, such as strength, durability, and resistance to environmental factors. It also provides key insights into the quality and workability of E3DCP. High homogeneity ensures that each layer of the printed object has consistent properties, which is essential for the overall stability and function of the structure. Particularly with innovative techniques like NNM, where the material mix is dynamically adjusted, ongoing homogeneity analysis enables precise control of the mixing process, contributing to high-quality end products. [Chr-2023]

2.4.1 Definition of Homogeneity

Homogeneity describes the state in which the components of a system or mixture are uniformly distributed, so that every taken subsample has the same composition as the entire system. In a homogeneous material, the physical and chemical properties are identical at all points, regardless of how small the considered sample is. This term is applied in various scientific disciplines, from chemistry and physics to materials science, geology, meteorology, etc.. In the context of materials and substances, homogeneity means that a substance consists of a single phase, without visible separations or layering of different materials or phases. [Bun-2016]

2.4.2 Methods of Homogeneity Analysis

Various methods are applied to analyze homogeneity, each with its own strengths and applications. One of the most basic approaches is visual inspection, which requires no specialized equipment and quickly provides initial impressions of the uniformity of a material. However, despite its simplicity, it is only suitable for rough assessment and may contain subjective biases. [Hil-2021] For a more detailed analysis, microscopic examination is appropriate, providing insights into the material structure at a microscopic level. This involves the use of light or electron microscopes to visualize the distribution of particles or phases within a sample. Microscopic analysis begins with the careful preparation of the sample to be examined. Depending on the material and the purpose of the investigation, various preparation techniques can be applied, including cutting, polishing, or specific staining methods to highlight certain structures. Once prepared, the sample is placed under a microscope. Various types of microscopes can be used depending on the analysis requirements. Microscopic examination can evaluate the homogeneity of a material by identifying inconsistencies such as agglomeration, phase separation, or uneven distribution of reinforcing fibers. This

information is crucial for optimizing material compositions, improving manufacturing processes, and ensuring the quality and reliability of products. [Mon-2021]

Spectroscopic methods, including Raman spectroscopy and infrared spectroscopy, expand the spectrum of analysis possibilities by capturing the chemical composition and molecular structure of materials. These techniques are particularly valuable for identifying the distribution of specific chemical compounds within a sample. [Bro-1991] Sieve analysis is commonly used to determine the particle size distribution in powders and granules. By passing the material through sieves with different mesh sizes, the distribution of particle sizes can be determined. Another method for analyzing particle size is laser granulometry, which utilizes the diffraction of laser light and is known for its speed and precision. [Mat-2023] Mechanical tests, such as measuring compressive or tensile strength, can also provide indications of the homogeneity of a material. Differences in the strength properties of different sample areas may indicate inconsistencies. Chemical analyses complement the spectrum of analysis methods by allowing a detailed examination of the molecular or elemental composition, conducted, for example, through chromatography or mass spectrometry. [Mon-2021]

Each of these methods contributes in its own way to assessing the homogeneity of a material and is suitable depending on the type of material and the specific analysis requirements. The selection of the appropriate method is crucial for the accuracy and reliability of the results.

2.4.3 Statistical Methods for Homogeneity Evaluation

Statistical methods play a crucial role in evaluating the homogeneity of materials and processes. They provide quantitative measures that allow for the objective analysis and interpretation of variability within a sample or a set of data points. [Sab-2002]

Two of the most common statistical measures used in homogeneity evaluation are the standard deviation (STD) and the coefficient of variation (CV). The standard deviation (STD) is a measure of the dispersion or variability of data points around their mean. In homogeneity analysis, it indicates how far individual measurements, on average, deviate from the overall mean. A low standard deviation means that the data points are closely clustered around the mean, indicating high homogeneity. Conversely, a high standard deviation suggests a wider spread of values and, therefore, lower homogeneity. The coefficient of variation (CV) is the ratio of the standard deviation to the mean, expressed as a percentage. It offers a standardized way to compare the relative variability of data sets with vastly different means. The CV allows assessing the dispersion independent of the magnitude of the measurements. A low CV indicates low relative

dispersion, suggesting high homogeneity within the sample or process, while a high CV points to greater variability and thus lower homogeneity. To effectively evaluate the homogeneity of a material or process, multiple samples or data points are often collected and analyzed. Calculating the standard deviation and coefficient of variation from these data provides objective, quantifiable measures of homogeneity. These measures can then be used to make decisions about product acceptance, process stability, improvements, or compliance with quality standards. [Ros-2013]

For instance, the use of STD and CV to analyze the homogeneity of the physical and chemical parameters of materials is employed. STD indicates how far the values in the dataset, on average, deviate from the mean, serving as a measure of the dispersion of material properties across the sample. CV normalizes the dispersion with respect to the mean, thus providing a comparable overview of relative variability, regardless of the magnitude of the measurements. Analysis using STD and CV is particularly valuable in the context of NNM. [Chr-2023] Integrating statistical methods into microscopic examination allows for an objective and quantitative analysis of material homogeneity on a microscopic level. This combination is especially useful for precisely assessing the distribution and size of particles, pores, phases, or other structural features within a sample. The collected microscopic images undergo quantitative image analysis. Using image processing software, features such as particle size, shape factors, pore size and distribution, and the area fractions of different phases can be quantified. This analysis results in a dataset that includes the measured values for each identified feature. [Mat-2023]

2.5 Programming Methodology

In this section delves into the programming methodology, particularly the utilization of Python (Section 2.5.1) in a Jupyter Notebook environment (Section 2.5.2). It also discusses useful libraries that are significant for data analysis and processing (Section 2.5.3). Python, as the programming methodology, takes center stage, being a versatile programming language used for data analysis and processing. The utilization of Jupyter Notebooks enables an interactive display of code, results, and explanations. Essential Python libraries such as NumPy, Matplotlib, Seaborn, OpenCV, and Pandas expand the capabilities for mathematical operations, visualization, image processing, and data management. This section outlines the technical foundations and tools necessary for conducting homogeneity analysis and image processing.

2.5.1 Python

Python is a high-level, interpreted programming language known for its clarity and simplicity in code. It was developed in the early 1990s by Guido van Rossum. Python supports multiple programming paradigms, including procedural, object-oriented, and functional programming, making it a versatile language that can be used in various application domains. One of Python's main features is its readable and concise syntax, which facilitates learning for beginners and encourages the development of efficient and maintainable codebases. The language utilizes simple English keywords and a minimal number of syntax rules, easing the entry for newcomers to programming. Python boasts an extensive standard library that provides modules and functions for a variety of tasks, such as file operations, system calls, network communication, and more. Overall, Python is a powerful and flexible programming language characterized by its simplicity, readability, and broad applicability. Its extensive ecosystem and strong community support make it a top choice for developers in many different domains. [Pyt-2024a]

2.5.2 Jupyter Notebook

Jupyter Notebook is an open-source web application that enables the creation and sharing of documents containing live code, equations, visualizations, and explanatory text. These interactive documents are called "notebooks" and support the execution of code in over 40 programming languages, including Python, R, and Julia. Jupyter Notebooks have become a valuable tool in areas such as data analysis, scientific research, information visualization, machine learning, and education. [Jup-2024]

Jupyter Notebooks allow for the interactive execution of code. Users can write code in individual executable cells and run this code in real-time to receive immediate feedback. This feature makes it ideal for exploratory data analysis and experimental development. They combine executable code with rich text, formulas (supported by LaTeX), images, and visualizations in a single document. This facilitates the creation of comprehensive tutorials, educational materials, and research reports covering both theoretical foundations and practical implementation. They can be easily shared, facilitating collaboration. They can be shared as email attachments, via GitHub, or using nbviewer online. Notebooks can also be exported to other formats such as HTML, PDF, Markdown, or Python code. From data cleaning and transformation to statistical modeling and data visualization to machine learning, Jupyter Notebooks provide a flexible platform for a variety of data science and research projects. Additionally, Jupyter supports numerous extensions that provide additional functionalities such as code and data visualization tools, presentation modes, and interactive widgets. [Jup-2024]

Jupyter Notebook consists of three main components: the Jupyter Notebook application, kernels, and notebook documents. The Jupyter Notebook application is a web application responsible for managing and presenting notebook documents. Kernels are separate processes launched by the Notebook application that contain and execute executable code. There is a specific kernel for each supported programming language. Notebook documents are the documents containing code, visualizations, and text. They are saved in JSON format and have a .ipynb file extension. [Jup-2024]

2.5.3 Useful Libraries

Python stands out for its rich ecosystem of libraries, providing developers with a wide range of tools for various application domains. These libraries cover a broad spectrum, from data analysis and scientific computing to machine learning, web development, and image processing.

For data analysis and scientific computing, NumPy, Pandas, and SciPy are indispensable. NumPy is a core library for scientific computing in Python, offering support for large, multi-dimensional arrays and matrices, along with a collection of mathematical functions to manipulate them. Pandas is a powerful, flexible, and easy-to-use open-source data analysis and manipulation library. It provides data structures like DataFrame and Series, specifically designed for working with structured data. Pandas is excellent for various data manipulation tasks, from simple tasks like reading data from different sources to complex data aggregations. SciPy builds on NumPy and extends its capabilities by providing many additional modules for optimization, linear algebra, integration, interpolation, special functions, FFT, signal and image processing, ODE solvers, and other tasks common in science and engineering. [Pyt-2024b]

For data visualization, Matplotlib, Seaborn, and Plotly are important tools. Matplotlib is a comprehensive library for creating static, animated, and interactive visualizations in Python. Matplotlib.pyplot is a collection of command-style functions that allow Matplotlib to work like MATLAB, providing a procedural interface to Matplotlib's object-oriented plotting library. It is particularly well-suited for creating 2D graphics and charts. With Matplotlib, users can create high-quality plots, histograms, power spectra, bar charts, and other types of charts with just a few lines of code. [Pyt-2024b]

For image processing, OpenCV (Open Source Computer Vision Library) and Pillow (PIL Fork) are essential. OpenCV is an open-source library for computer vision and machine learning. cv2 is the Python wrapper for OpenCV, offering extensive functions for image and video processing. With cv2, developers can perform tasks like face recognition, object detection, image segmentation, and much more. [Pyt-2024b]

The `os` library in Python belongs to the area of system programming and operating system interaction. `os` is a module in the Python standard library that provides a simple way to interact with the operating system. It contains functions for file and directory management (e.g., creating, deleting, or modifying paths), accessing environment variables, starting processes, and more. `os` enables scripts to work portably across different operating systems. [Pyt-2024b]

In the field of machine learning and artificial intelligence, libraries like Scikit-learn, TensorFlow, and PyTorch dominate. And in web development, Django and Flask offer robust solutions. Finally, BeautifulSoup and Scrapy are excellent tools for web scraping. [Pyt-2024b] This diversity of libraries is a key aspect that makes Python a preferred choice for developers in numerous disciplines, enabling the development of efficient, powerful, and flexible applications.

2.6 Image Analysis Techniques

This section deals with image processing methods essential for examining the homogeneity of mortar mixtures. This includes grayscale conversion (Section 2.6.1), noise reduction methods (Section 2.6.2), various thresholding techniques (Section 2.6.3), and morphological operations (Section 2.6.4), each explained in detail.

2.6.1 Grayscale Conversion

Grayscale conversion is a fundamental step in image processing and plays a crucial role in digital image analysis, especially when color information is not required for the specific task or when simplifying the analysis. A color image consists of multiple channels (typically red, green, and blue) that together produce the various colors of the image. In contrast, a grayscale image has only one channel, representing different shades from black to white, with each pixel value indicating the brightness at that point. Using grayscale conversion as the first step in image processing is advantageous. This step can initially reduce the complexity of the image by decreasing the amount of data to be processed. It also focuses the analysis on the luminance (brightness information) of the image. Additionally, it reduces the computational and storage requirements, which is particularly advantageous for large image datasets or real-time applications. [Sar-2010]

There are generally two methods of grayscale conversion: the direct method and the weighted method (luminance method). In the direct method, the average of the three-color channels (red, green, blue) is taken to determine the grayscale value of each

pixel (Section Equation (2-1)). However, this method does not consider the different sensitivity of the human eye to these colors. [Sar-2010]

$$Grauwert = \frac{R + G + B}{3} \quad (2-1)$$

Weighted method, also known as luminance method, considers human color perception by assigning different weights to the color channels (Section Equation (2-2)). For example, green contributes more to perceived brightness than red and blue. [Sar-2010]

$$Grauwert = 0.299R + 0.587G + 0.114B \quad (2-2)$$

These weightings reflect the varying sensitivity of the human eye and provide a more realistic result in terms of perceived brightness. Grayscale conversion often forms the initial step in the image processing pipeline and lays the groundwork for many subsequent analyses by reducing an image to its essential brightness information.

2.6.2 Noise Reduction

Noise reduction in image processing involves minimizing unwanted noise in images to improve their quality and make them more accessible for further analysis. Various sources, including image sensors, poor lighting, or transmission errors, can lead to image noise, which complicates image interpretation in areas such as medical imaging or satellite photography. There are several types of noise, including Gaussian noise with its characteristic normal distribution across pixels, salt-and-pepper noise, characterized by random black and white pixels, and speckle noise, which occurs mainly in radar and ultrasound images. [Sab-2002]

To mitigate this noise, diverse strategies have been devised. Linear filters, such as the Gaussian low-pass filter, are effective against Gaussian noise but tend to smooth out important image details. Non-linear methods, such as the median filter, effectively remove impulse noise by using the median values of the pixel neighborhood. Furthermore, wavelength-based approaches through wavelet transformation provide differentiated processing of different frequency components, allowing for targeted noise reduction. Bilateral filters and anisotropic diffusion (Perona-Malik filter), on the other hand, preserve image edges and details by performing smoothing depending on the spatial and intensity-based context of the image. [Sab-2002]

The challenge in noise reduction lies in finding a balance between suppressing noise and preserving essential image information such as edges and textures. Modern

research efforts, including the application of machine learning and deep learning techniques, aim to optimize this balance and further improve the effectiveness of noise reduction. [Sab-2002]

2.6.3 Thresholding Methods

The thresholding method, also known as thresholding, is a simple yet effective technique in image segmentation, aimed at separating objects or features in digital images. It relies on selecting a specific intensity value (threshold) and classifying pixels based on whether their intensity is above or below this value. The goal is to segment the image into meaningful regions that can be isolated for further analysis. Based on this check, the pixels are then assigned to one of two possible classes: foreground (object) or background. The most basic form of the thresholding method is binary and follows this simple rule. First, if the pixel value is greater than the threshold value, the pixel is assigned to the foreground (usually set to white or the maximum intensity value). Second, if the pixel value is less than or equal to the threshold value, the pixel is assigned to the background (usually set to black or zero). [See-2023]

There are various methods to determine the optimal threshold value for an image, including global thresholding, adaptive thresholding, and Otsu's method. In global thresholding, a single threshold value is used for the entire image. This is effective for images with good contrast between foreground and background. In adaptive thresholding, the threshold value is calculated locally for smaller image regions, which is helpful when the lighting conditions vary within the image. Otsu's method is an automatic and widely used technique for threshold determination in digital image processing, aiming to find the optimal threshold value for separating foreground and background in an image. The method is based on a simple principle: it seeks the threshold value that minimizes the variance within classes, which is equivalent to maximizing the variance between classes. When performing this method, first, the histogram of the grayscale image is computed. The histogram shows the frequency distribution of pixel intensities in the image. Then, the histogram is normalized, dividing each intensity value frequency by the total number of pixels. This transforms the histogram into a probability distribution of intensities. With this data, calculations of cumulative sums and variances are performed. In calculating the cumulative sums, for each possible threshold value t , two cumulative sums are computed: the cumulative sum of class probabilities up to t and the cumulative sum of class probabilities multiplied by the corresponding intensity values (for the mean). The formula below illustrates this calculation. For each possible threshold value t , the following is computed: [See-2023]

Cumulative probability $P_1(t)$ for the background (class 1):

$$P_1(t) = \sum_{i=0}^t p(i) \quad (2-3)$$

where $p(i)$ is the probability of the occurrence of intensity i in the histogram. Cumulative mean $\mu_1(t)$ for the background (class 1):

$$\mu_1(t) = \sum_{i=0}^t i \cdot p(i) / P_1(t) \quad (2-4)$$

This calculates the mean of the pixel intensities for the background up to the threshold t , weighted by the desired probability. This is followed by the calculation of the variances. For each possible threshold t , the variances within the classes and the variance between the classes are calculated. The variance between classes is a measure of how well two separate groups can be distinguished. The computational steps are shown with the formulas below: [See-2023]

To maximize the variance between classes, it is calculated for every possible threshold t :

$$\mu_T = \sum_{i=0}^{L-1} i \cdot p(i) \quad (2-5)$$

Here, μ_T is the overall mean, and L is the number of possible intensity levels in the image.

$$\sigma_B^2(t) = P_1(t) \cdot (1 - P_1(t)) \cdot (\mu_1(t) - \mu_T)^2 \quad (2-6)$$

Here, $P_2(t)$ and $\mu_2(t)$ represent the cumulative probability and the cumulative mean for the foreground (class 2), respectively. The threshold t is chosen to maximize $\sigma_B^2(t)$. This threshold effectively separates the foreground from the background by maximizing the variance between these two classes. It is selected as the optimal threshold for segmentation. The found optimal threshold is then applied to the grayscale image to assign each pixel either to the foreground or the background, based on whether its intensity value is above or below the threshold. [See-2023]

2.6.4 Morphological Operation

Morphological operations are basic tools in image processing aimed at the shape of structures within an image. They are commonly used in image segmentation to edit and analyze images based on their morphological features. These techniques are particularly well-suited for processing binary images but can also be applied to grayscale images. The operations are based on mathematical morphology and use structural elements (also known as kernels or masks) to process specific shapes within an image. [Soi-2004]

The most commonly used morphological operations include erosion, dilation, opening, and closing. Erosion removes the outer pixels of objects in an image, resulting in the shrinkage of the objects. This operation is useful for eliminating small disturbances and separating objects when they slightly overlap. Practically, this is achieved by retaining only those pixels whose neighborhood is completely within the object, based on the used structural element. Dilation, on the other hand, adds outer pixels to the objects in an image, enlarging these objects. This operation can be used to fill small holes or cracks within the objects and bring separate objects closer together. Dilation achieves this by adding pixels that overlap with the structural element. Opening is an operation performed by the sequence of erosion followed by dilation. It is effective in removing small objects or outliers while preserving the shape and size of the larger objects in the image. Opening can also help separate the objects from one another and smooth their contours. Closing is the counterpart to opening and is performed by applying a dilation followed by erosion. This operation is useful for filling small holes or cracks within the objects and connecting separate objects without significantly changing the size of the larger objects. [Soi-2004]

These morphological operations are powerful tools for image segmentation, as they allow objects to be isolated, removed, or highlighted based on their shape. They are used in a variety of applications, from medical image analysis to traffic monitoring, and are essential for tasks where the shape and structure of objects matter. By adjusting the structural element, these operations can be tailored to specific requirements, offering great flexibility in practical application.

3 Analysis and Classification of NNM in AM for Concrete Construction

This chapter offers a thorough analysis and structured classification of Near Nozzle Mixing (NNM) within the context of Additive Manufacturing (AM) for concrete construction (AMC) (Figure 3-1), drawing on the research introduced in section 2.1 through 2.3. The classification focuses on delineating the role of the NNM process in AMC while encompassing the broader scope of AM technologies.

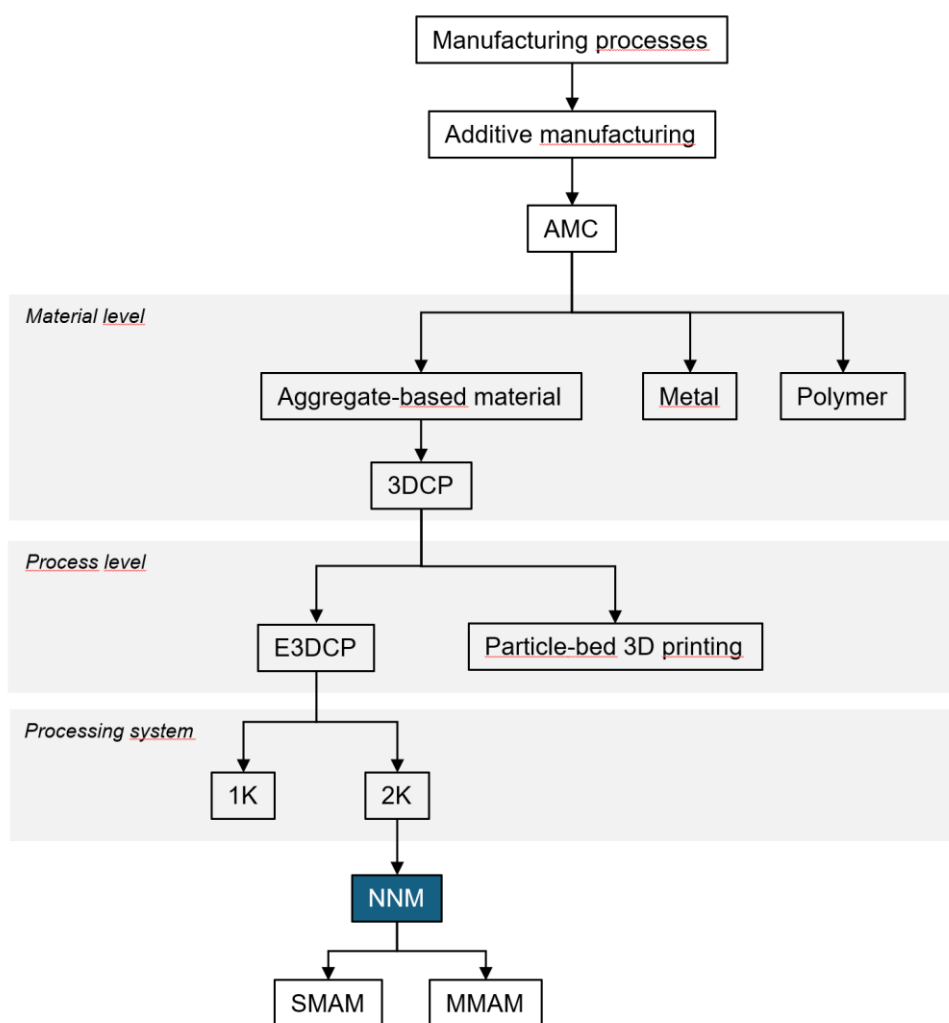


Figure 3-1: Process classification of NNM process

As outlined in section 2.3.5, NNM aims to optimize the composition of concrete materials immediately before their extrusion through the nozzle [Chr-2023]. The classification framework begins by categorizing manufacturing processes, with a specific emphasis on AM processes tailored for construction applications. More detailed

classifications of manufacturing processes (Figure 2-1), AM processes (Figure 2-2) and AMC processes (Figure 2-4) can be found in section 2.1 and 2.2, respectively. AMC can be classified in various ways, considering criteria such as the material used, printing technology, application area, construction size, degree of automation, and others [Gib-2021]. Given the focus of NNM on concrete-based AM processes, the initial classification criterion is based on the material. In addition to aggregate-based materials, metals and polymers are also significant areas of research in AMC [Pac-2021]. Concrete serves as the primary focus within aggregate-based materials in construction, referred to as 3DCP (Section 2.2). Under 3DCP, various processes are utilized for 3D printing, with E3DCP (Section 2.3) and particle-bed 3D printing (Section 2.2.1) being the most prominent processes. However, NNM remains primarily associated with E3DCP.

Wangler's study introduces the concept of a 1-component system (1K) and a 2-component system (2K) (see 2.3.1). These denote the number of components or materials used in E3DCP. A 1K system employs only one component or material for the printing process, whereas a 2K system utilizes two components or materials, either mixed to achieve different properties or extruded simultaneously for complex structures or multi-color prints [Wan-2022]. NNM involves combining the dry and liquid components of concrete shortly before deposition [Chr-2023]. This notable characteristic underscores the importance of classifying the processing system, with NNM being categorized under the 2K system. Furthermore, NNM is further classified into NNM single-material AM and multi-material AM (MMAM) (Section 2.3.3), illustrating its adaptability to both AM approaches. As highlighted in 2.3.5, NNM technology serves as a cornerstone for advancing multi-material printing, allowing for material composition adaptation during the printing process [Chr-2023]. Additionally, as discussed in section 2.3.3, single-material AM refers to using a single material for the entire printing process, while MMAM involves using multiple materials, either simultaneously or sequentially, to produce components with different properties or functions. Thus, it is logical to classify both single-material AM and MMAM under the NNM process.

In conclusion, the classification of NNM process in AMC presents a structured framework that offers several advantages. It facilitates a systematic understanding of NNM's principles and applications, enhances communication and collaboration within the research community, and enables comparisons with other AM processes. However, there are challenges such as the risk of oversimplification and the need for ongoing updates to accommodate technological advancements. Despite these limitations, the classification framework provides valuable insights into NNM's role in AMC and serves as a foundation for future research and development in the field.

4 Homogeneity Analysis and Mix Quality Evaluation in NNM with GRES V1.3

This chapter focuses on the homogeneity analysis for evaluating the mix quality of the NNM system conducted by the developed GRES V1.3. Section 4.1 describes the conduct of experiments with GRES V1.3, including recipe adjustments to produce a printable mortar mixture. Section 4.2 illuminates the sample preparation process, starting from the extraction after the experiment to processing and capturing micrographs. The image processing methods are presented in Section 4.3, followed by a statistical analysis of the collected data in Section 4.4. Finally, the results will be interpreted in section 4.5, offering insights into the mix quality of the NNM system and highlighting potential areas for improvement.

4.1 Experimental Procedure

The evaluation of mix quality within the realm of NNM necessitates precise and systematic experimental execution, laying the groundwork for subsequent homogeneity analysis. At the heart of this process lies the GRES V1.3 (section 2.3.6), purposefully designed to meet the requirements of NNM and mounted on a KUKA robotic arm to ensure optimal precision and flexibility. The objective is to consistently produce printable mortar. The experimental procedure, developed based on Wangler's study of digital concrete processing (section 2.3.1), is divided into five main phases. Firstly, the mix proportioning phase (section 4.1.1) entails the preparation of recipes for the cement paste and Poraver, establishing the qualitative and quantitative foundations for the desired mixture, which is pivotal for result consistency. Subsequently, in the primary mixing phase (section 4.1.2), the cement paste undergoes a meticulous mixing process where careful selection of mixing parameters ensures the creation of a homogeneous base for the printable mortar. The third phase involves storage (section 4.1.3), where interim storage and consistency maintenance of the adhesive demand accurate monitoring to uphold consistent material quality. Finally, the fourth and last phase encompasses transport and secondary mixing (section 4.1.4), where the cement paste, along with the Poraver mixture, is conveyed into the mixing area of the GRES V1.3. This step is pivotal for achieving homogeneity in the final mixture, as it involves thorough mixing of the components. The meticulous execution of these phases is paramount in producing a high-quality mixture for NNM and serves as the basis for subsequent analysis of sample homogeneity.

Before commencing this experimental procedure, system setup and calibration must be conducted to ensure a smooth and accurate process. This involves configuring and calibrating the GRES V1.3 (Figure 4-1) and preparing all necessary components for the mixing and printing process. Tasks include installing the cement paste mixer, setting up the intermediary station for cement paste storage, configuring the paste pump, constructing the mixing area, and providing containers for residual cement paste and mortar. Additionally, equipment for the spread test, a method for assessing cement paste and mortar consistency according to DIN EN 1015-3, should be prepared.

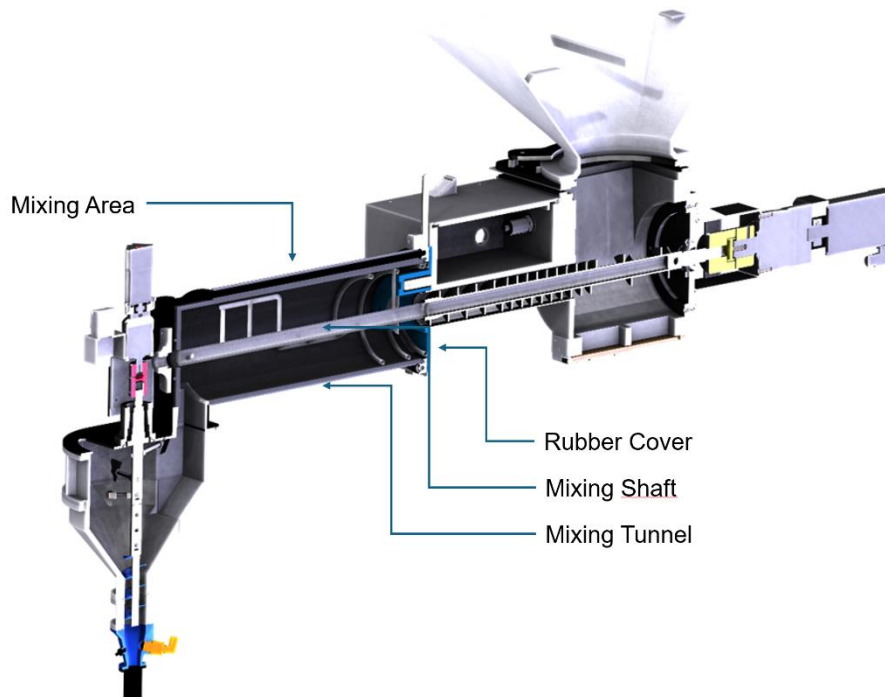


Figure 4-1: Cross-section of the current prototype GRES V1.3, Credit_ Maximilian Dahlenburg, TUM

The PFT forced mixer MULTIMIX serves as the central element for blending the cement paste, boasting a batch capacity of 80L. Positioned near the storage station, it facilitates the smooth transfer of the paste. Additionally, an electric mortar mixer is on standby to provide manual supplementary energy during the mixing process. The storage station comprises a barrel with a minimum capacity of 80L and a large electric mortar mixer installed, featuring a mixing tool that reaches nearly to the bottom. A metal pipe serves as the conduit to connect the paste pump. The paste pump is equipped with PVC hoses with a $\frac{1}{2}$ inch inner diameter. While the inlet hose links the pump to the storage station, the outlet hose directs to the mixing area. Before the test, the flow rate (L/min.) of the pump and hoses is calibrated to detect potential blockages early. The mixing area features a rubber cover at the connection point to the mixing shaft, the mixing shaft itself, and a mixing tunnel. These components are disassembled, cleaned, and reassembled before each use. The containers for residual materials are required to be large and robust. To prevent hardening, they are treated with form oil.

For conducting the spread test of the cement paste, a set comprising a glass plate, settling funnel, and ruler is utilized. Meanwhile, for mortar, a Hägermann spread table, settling funnel, and tamper are employed to assess flow properties.

4.1.1 Mixing Proportioning

The choice of Lightweight Mortar (LWM), composed of cement paste and Poraver, as the material for this study is pivotal. The development and preparation of an accurate recipe for cement paste and Poraver represent a critical starting point for research in the field of 3DCP. A well-defined recipe ensures not only the quality and buildability of the printing material but is also essential for the homogeneity and structural integrity of the printed object. The recipe used in this phase, based on insights from the studies by Hechtl (Section 2.3.7) and adapted for the specific requirements of the NNM technique with the GRES V1.3 system.

The mortar for the experiments consists of two main components: cement paste and Poraver. Cement paste serves as the binder that forms the structural basis of the mortar. It significantly contributes to the strength, buildability, and durability of the final product. Through its flow properties, the cement paste enables an even mixing of components and a smooth extrusion through the nozzle system of GRES V1.3. As introduced in section 2.3.7, Poraver particles are used in four different size: 0.1-0.3 mm, 0.25-0.5 mm, 0.5-1.0 mm, and 1.0-2.0 mm. The mixing of Poraver particles is done according to specified mass fractions to ensure a homogeneous composition (Table 4-1):

Table 4-1: *Recipe for Poraver mixture*

Particle Size [mm]	Mass Fraction [%]	Weight per Mixture [g]
0.10 – 0.30	34.39	6174
0.25 – 0.50	24.26	4343
0.50 – 1.00	18.15	3249
1.00 – 2.00	23.10	4136

For the mixing process of Poraver mixture, a drum mixer is used to achieve an even distribution of Poraver particles of different sizes. This mixing process involves tilting the drum mixer approximately 45 degrees to the left and right, with each side being mixed for about 3 minutes. This process ensures that all particle sizes are distributed evenly throughout the volume. Due to the container and drum mixer's capacity limitations, each mix is performed with the specified weights of the various Poraver particle size ranges. For conducting an experiment, the mixture is prepared 2-3 times.

The basic recipe for the cement paste, based on Hechtl's study (Section 2.3.7), is further developed (Table 4-2). For improved image contrast detection, the basic recipe is additionally adjusted with red pigments (Table 4-3). This adjustment aims to enable a clear contrast between Poraver and the cement paste during processing, thus simplifying the homogeneity analysis. The composition of the cement paste and the specific mass proportions of each component for a total volume of 75.65 L of cement paste, which corresponds to the amount for one experiment, are defined as in Table 4-2.

Table 4-2: *Basic Recipe for Cement Paste Mixture*

Component	Mass Fraction [%]	Weight per Trial [g]
Water	20.17	29160.96
Superplasticizer (MasterGlenium ACE 460)	0.40	581.29
Silica Suspension (Sika Silicoll SL)	15.08	21797.75
Cement (Portland Cement EN197-1)	62.13	89796.70
Limestone Powder	2.51	3633.02

Based on the basic recipe for cement paste, 1% of the cement mass of red pigments is added. To maintain the balance between dry and liquid components, adjustments are made as follows: The mass of the pigments is deducted from the silica suspension, doubling the amount. Since the silica suspension consists of 50% water and 50% silica dust, the adjustment is divided accordingly. Silica fume is substituted to minimize changes in the gradation curve, as pigments, like silica fume, belong to the finest particles in the mixture and are very similar. To compensate for the reduction in the silica suspension, an equal mass of water is added. The adjusted recipe is presented in Table 4-3.

Table 4-3: *Adapted Recipe for Cement Paste Mixture with Red Pigments*

Component	Weight per Trial [g]
Water	30058.92
Superplasticizer	581.29
Silica Suspension	20001.81
Cement	89796.70
Limestone Powder	3633.02
Red Pigment	897.97

The recipe adjustment aims to improve the visual distinction between Poraver and cement paste without disturbing the overall balance of the mortar. By reducing the silica suspension and adding water, it ensures that the consistency of the cement paste and thus its printability is maintained. The dry components are carefully weighed before the test day and stored in climate controlled container to ensure their quality.

4.1.2 Primary Mixing

Following the mixing proportioning step, the primary mixing of the cement paste begins, a process that requires thorough preparation and meticulous execution. Initially, it is ensured that the cement paste mixer is free of any residues such as dust or concrete remains to maintain the purity of the new mortar. Subsequently, the mixer is activated, and the liquid components – water, superplasticizer, and silica fume suspension – are added. To achieve efficient use of materials, it is advisable to first add half of the water to the mixer. The remaining water is used to rinse out any remaining superplasticizer and silica suspension from their container, thus ensuring complete utilization of the precisely weighed materials in order to maintain the sensitive cementitious system. During this process, an empty container should be placed under the opening to catch any dripping liquid and return it to the mixer. After all liquid ingredients have been added, the mixer runs for about a minute to evenly distribute the temperature throughout the mixture. The addition of dry materials, starting with cement, followed by limestone powder, and the pigments. From this moment, the official mixing time begins. After adding all components, the mixture is further mixed for about two minutes. After that, the mixer is turned off, larger lumps are manually broken down, and the mixture is mixed at the highest speed with the handheld mortar mixer for another two minutes to break agglomerations of the fine particles such as silica fume, pigments and cement. Because the agglomerates influence the flow behavior of the paste. The material will be more fluid than originally planned in the design, as the cement necessary for hydration is not fully released. After this phase, the large mixer is activated again until a total mixing time of 30 minutes is reached. To conclude, a further treatment with the handheld mortar mixer at the highest speed for approximately two minutes is carried out.

4.1.3 Storage

After the primary mixing is completed, the cement paste is immediately transferred manually to an storage station. This step is crucial to continuously stir the paste and prevent it from drying out. During the transfer process, the large handheld mortar mixer at the storage station remains activated at level 2 to ensure a uniform consistency of the paste. Simultaneously, the ongoing paste mixer and mortar mixer at the storage station ensures that the paste is continuously stirred even during the transfer. For

transferring the paste, it is channeled through the mixer's opening into a portable container, with a grid sieve retaining larger material grains. Although the previous mixing process should have already ensured high homogeneity, the sieve helps to remove any remaining large particles. The sieved paste is then transferred multiple times to the storage station using the portable container until the paste mixer is completely emptied.

Immediately after transferring, a spread test is conducted to check the consistency of the paste (Section 2.3.7), aiming for a diameter of 350mm to 390mm. If the diameter is too large, a thixotropic agent is added to adjust the consistency. Thixotropic agents alter the rheological properties of the paste by increasing the viscosity and thus reducing flowability [Kru-2019]. The thixotropic agent is added in amounts of first 2g and then, if necessary, in further increments of 0.5g, with the mixer being increased to level 3 and the paste stirred for an additional 2 minutes after each addition. Once the desired consistency is achieved, the mixer can be turned down to the lowest level (level 1) to keep the paste at a consistent consistency until use. For long-lasting experiments, it is necessary to periodically repeat the spread test to ensure that the paste continues to meet the requirements and remains ready for use. This careful monitoring and adjustment of the paste's consistency are crucial for the quality and printability of the final mortar.

After the paste has been successfully transferred to the storage station, it is critical to promptly clean the mixer and all used equipment. This step is necessary to prevent remnants of the paste from drying out and hardening into concrete, which could damage the devices and affect future mixing processes. Immediate cleaning ensures the functionality and longevity of the equipment and ensures a consistently high quality of the mixing process.

4.1.4 Transport and Secondary Mixing

Following the preparation of the cement paste, the pivotal phase of the experimental procedure with the GRES V1.3 begins - the transport of cement paste to GRES V1.3 and secondary mixing with Poraver mixture in the mixing area (Figure 4-2). This is accomplished through a calibrated pump that supplies the cement paste, while the Poraver mix is introduced via a hopper mounted on top of the GRES V1.3. Through precise control of the pump frequency (Hz) and the mixing shaft motor's speed (rpm), the ratio between the volume share of Poraver and cement paste can be optimally adjusted.

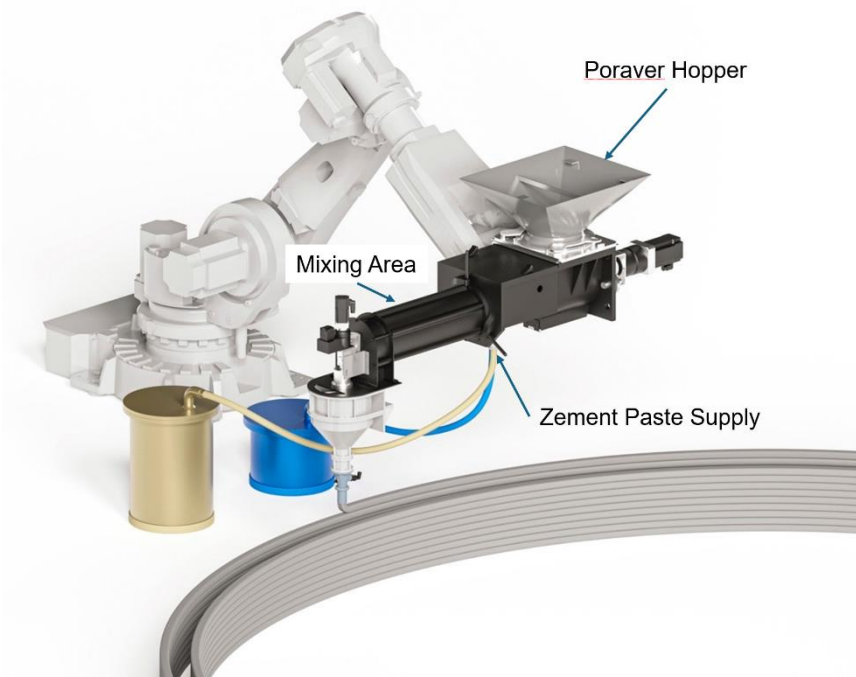


Figure 4-2: Rendering of GRES V1.3 in periphery, Credit cbm, fml TUM, P. Schneider

Precise calibration is necessary before the start of the experiment to accurately determine the flow of cement paste and Poraver. The calibration of the cement paste pump is carried out by setting frequencies in increments of 10, from 10 to 80 Hz, with the flow measured over one minute and repeated three times for each setting. From these measurements, the average flow per Hz is calculated. Similarly, the mixing shaft motor is tested in increments of 10, from 10 to 100 rpm, and the Poraver flow is measured three times to determine the average flow in L/rpm. The calibration results dictate that at a setting of 90.44 rpm for the mixing shaft motor, a Poraver flow of 3.6 L/min is necessary. For the cement paste pump, a flow of 1.8 L/min is set at 38.31 Hz, allowing for a ratio of 2.0. This ratio results in a mortar with a spread diameter between 125-135mm, which is considered optimal for the printing process and ensures a printable mortar quality. The spread test with mortar (Section 2.3.7) is an essential procedure to determine the fluidity and thus the workability of the mortar. Ideally, the printable mortar

should achieve a spread diameter between 125mm and 135mm. Values within this range indicate good fluidity, which is crucial for processing in the 3D printing process. Should the spread diameter fall outside this range, adjustments can be made to the mortar composition to achieve the desired consistency. With the successful completion of the experimental series, a profound understanding of the NNM process using the GRES V1.3 system has been achieved. By repeatedly conducting these experiments and performing targeted homogeneity analyses at various points within the mixing area, the distribution of Poraver particles in the mortar during the mixing process can be precisely examined.

4.2 Sample Preparation

The preparation and analysis of mortar samples is a crucial step in assessing the homogeneity and quality of 3D concrete printed with the GRES V1.3 system. This process begins with the accurate extraction of samples immediately after the printing process to create a representative basis for analysis (Section 4.2.1). Subsequently, sample processing (Section 4.2.2), which involves cutting and treatment with color enhancer, ensures optimal surface quality for microscopic examination. The final phase, the thin section imaging (Section 4.2.3), allows for detailed insights into the mortar's microstructure, especially the distribution of Poraver particles, through high-resolution microscope images.

4.2.1 Sample Collection

The effective sample collection is essential to conduct a comprehensive homogeneity analysis of the mixing quality within the mixing area of the GRES V1.3 system. The objective is to collect samples across the entire mixing area, from the beginning to the end, to enable a detailed assessment of material distribution. The mixing area has the length of 525 mm. For detailed examination of the mixing process, a Discrete Element Method (DEM) simulation was conducted by Jiayi An's study [Jia-2023], enabling a clear visualization of the mixing operation (Figure 4-3).

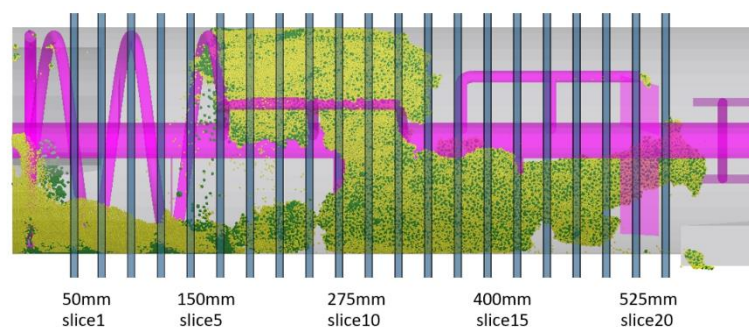


Figure 4-3: Position of the grid bin for evaluating the mixing performance [Jia-2023]

One implemented method for sample collection involves creating an opening at 16 cm from the mixing area's bottom, through which the remaining materials can be extracted when the system is stopped (Figure 4-4). This allows for obtaining a sample of 35-45 cm in length. This method offers the advantage that multiple mixing areas for separate samples do not need to be constructed.



Figure 4-4: Sample extraction from the mixing zone: 435 mm in length, starting at 160 mm

The alternative approach is to modify the system to extract samples with varying mixing area lengths. These samples will be placed in 3 Gang Mortar Prism Moulds and dried. The clear advantage of this method is that the end product directly provides insights into the effectiveness of the implemented changes. The downside is the significantly higher effort required for preparation and execution (Figure 4-5).

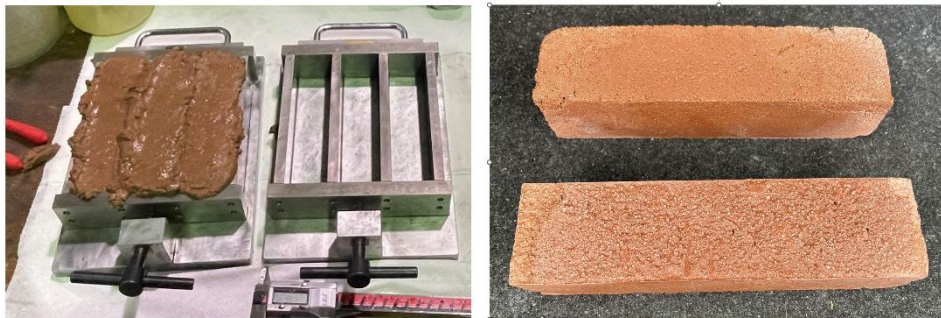


Figure 4-5: Left: Sample extraction from the end product; Right: Dried and demolded sample.

Both approaches to sample extraction contribute to gaining valuable insights into the mixing dynamics and material distribution within the GRES V1.3 system. Combining both methods is also helpful for comparing evaluations with each other.

4.2.2 Sample Processing

The processing of mortar samples is a crucial step in preparing the samples for subsequent microscopic examination and homogeneity analysis. The focus lies on two main procedures: cutting the samples and applying a color enhancement to increase the contrast between the different material components. While grinding and polishing are traditionally standard procedures in sample preparation, they are omitted in this particular case. The reason for this lies in the specific nature of the Poraver. Grinding

and polishing could damage the surface of the lightweight Poraver particles, leading to undesirable smudging of the color and thus distorting the analysis results.

After the drying process, the mortar samples are first cut. This process requires precision to ensure that the cuts are accurate and clean, which is crucial for a representative analysis of the material composition within the mixing area. For this precise processing of the mortar samples, a wet cutting machine (Figure 4-6) is used. This method is particularly suitable for ensuring water cooling during cutting, preventing overheating and potential damage to the sample. Special attention is paid to maintaining a maximum sample height of 5 cm to ensure compatibility with the requirements of microscopic examination and to allow for sample maneuverability under the microscope. Both surfaces of the sample should be cut as horizontally flat as possible. This precision in cutting ensures a flat surface, which is better suited for reducing microscopy processing time.



Figure 4-6: Left: Wet cutting of samples in cubic meters at Centrum Baustoffe und Materialprüfung; top right: Cut samples from the end product; bottom right: Cut samples from the mixing zone.

To improve the visibility and distinguishability of Poraver from cement paste in the mortar (Figure 4-7), a matte color enhancement is applied. This involves using a specially formulated color solution that penetrates into the pores and micro-cracks of the sample without altering the material structure. This method significantly enhances the contrasts under the microscope, thus facilitating the identification of the different phases within the mortar.



Figure 4-7: Comparison between untreated and color-enhanced samples.

The adjustment and standardization of sample processing methods are critical factors in achieving valid and meaningful results in homogeneity analysis. Consistency in sample preparation ensures that all samples are analyzed under identical conditions, thereby ensuring the comparability of results across different samples. This is particularly important because even minor deviations in the preparation process can lead to significant differences in the analysis results. By adhering to a consistent method of processing, including cutting, color enhancement, and potentially other steps, the groundwork is laid for a reliable assessment of mortar homogeneity.

4.2.3 Cross-Sectional Image Acquisition

The acquisition of grinding images is a crucial step in the analysis of the homogeneity of mortar samples, enabling a detailed examination of the material distribution within the sample. These high-resolution images are essential for assessing the quality and uniformity of the material.

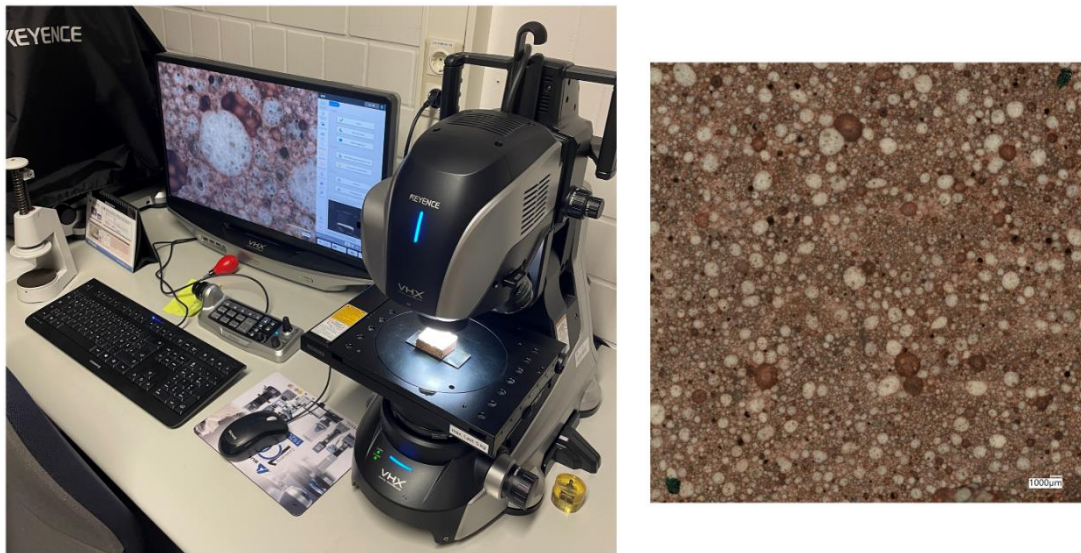


Figure 4-8: Left: Keyence VHX digital microscope at the Institute for Machine Tools and Industrial Management; right: Captured cross-section image

For the acquisition of grinding images, the Keyence VHX digital microscope is used (see Figure 4-8). This advanced microscope system is characterized by its high resolution, excellent image quality, and user-friendliness. It allows for detailed examination of the sample structure at various magnification levels.

A critical aspect of grinding image acquisition is the scaling within the image, which is essential for quantitative analysis. The standard magnification for capturing these grinding images is x80, providing sufficient depth of detail to examine the distribution of Poraver particles in the adhesive accurately. If the sample is flat and even enough, the microscope allows for capturing with a uniform focus across the entire sample. However, for samples with uneven surfaces, the use of the autofocus function with depth of field is necessary, provided by an internal function of the digital microscope used in this study. Although this process takes considerably more time, it ensures that all areas of the sample are captured sharply and in detail.

Another important feature is the series capture, where multiple images of a sample surface are automatically stitched together into a single, seamless cross-sectional image. This technique is particularly useful for examining larger sample areas and ensures that the entire investigated surface is captured in high resolution without any loss of information.

4.3 Image Processing

In this chapter, the essential phase of image processing is explained, which is indispensable for the precise analysis of mortar sample homogeneity. This structured phase consists of several key steps that enable the extraction of detailed and meaningful information from the grinding images.

The first step, image preprocessing, described in section 4.3.1, involves converting the images to grayscale and reducing noise to optimize the image quality for subsequent analysis. These techniques are fundamental to enhancing contrasts and minimizing undesirable noise, enabling more precise segmentation and analysis. In the second step, image segmentation, described in section 4.3.2, the thresholding method using Otsu's method is applied to separate the relevant features from their background. In cases where specific manual adjustments are required, a global thresholding method may also be employed. To further refine the segmentation results, morphological operations are applied to define the structure and boundaries of the identified objects more clearly.

The final step, validation of image processing (see 4.3.3), involves reviewing the processed images to ensure their suitability for statistical analysis. In this phase, it is assessed whether the image processing techniques conducted have led to meaningful and analyzable results.

4.3.1 Image Preprocessing

The first step of image processing in the homogeneity assessment of mortar is image preprocessing. This section focuses on two central aspects of image preprocessing: converting the images to grayscale and reducing noise, with noise reduction being an optional step. Converting the colored images to grayscale is a fundamental step that reduces the complexity of the image information and simplifies subsequent image processing. By focusing on brightness values rather than color information, grayscale conversion enables more efficient segmentation and analysis of structures within the sample. This technique is particularly important for examining the distribution and homogeneity of materials such as Poraver and adhesive in the mortar.

As described in section 2.6.1, there are two methods for grayscale conversion: direct method and weighted method. The weighted method is chosen for converting the mortar samples to grayscale because it considers the varying sensitivity of the human eye to the colors red, green, and blue. This method is particularly advantageous for analyzing samples consisting of red adhesive and white Poraver particles. It maximizes the contrast between the red adhesive and white Poraver particles in the grinding images of the samples, which is essential for subsequent image analysis and processing to enable precise identification and segmentation of the particles. The method enhances the visibility of material differences, facilitating accurate assessment of Poraver distribution homogeneity in the mortar. The OpenCV library (Section 2.5.3) enables the conversion of color images to grayscale using Python (Section 2.5.1) and is visualized using Jupyter Notebook (Section 2.5.2). This conversion internally utilizes the weighted method, the details of which are provided in Appendix A. The conversion is illustrated in Figure 4-9.

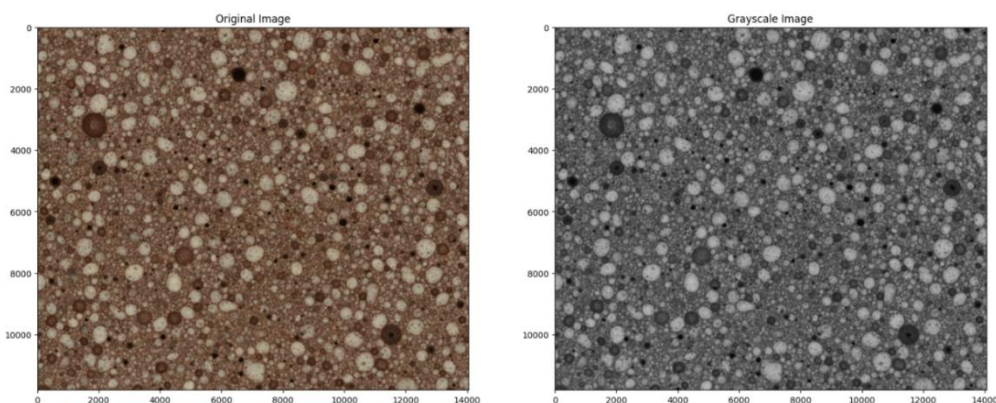


Figure 4-9: Comparison between original image and grayscale image.

Digital images are often affected by various types of noise, which can degrade image quality and make analysis difficult. Applying noise reduction techniques, such as Gaussian blur, median filter, or bilateral filter, enhances image clarity by minimizing distracting artifacts and background noise. Careful noise reduction is crucial for increasing the precision of subsequent image segmentation and analysis and facilitating the identification of relevant features.

In the basic script (Appendix A), three noise reduction methods, Gaussian blur, median filter, and bilateral filter, are employed (Section 2.6.2) to optimize image quality for analysis. Each of these methods has specific characteristics that make them suitable for different types of image noise and analysis requirements. The choice of the appropriate noise reduction method depends on the specific nature of the noise and the goals of the image analysis.

An example is shown in Figure 4-10, where the detected Poraver surfaces are marked by green contours. While Gaussian blur and median filter are widely used, the bilateral filter provides an excellent solution for applications where preserving edges and details is crucial. The combination of these techniques allows for flexible adaptation to the challenges of image preprocessing, creating the best possible conditions for subsequent image segmentation and analysis.

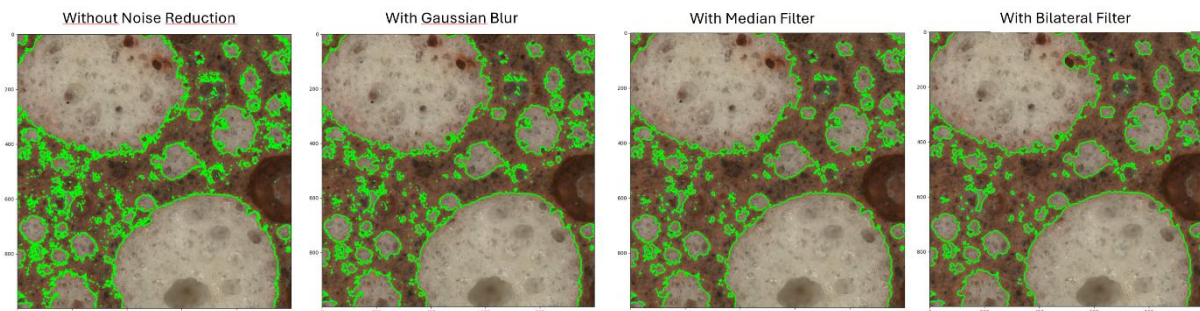


Figure 4-10: Comparison between using different noise reduction methods

Performing these image preprocessing steps lays a solid foundation for the detailed examination of the sample. Through this conversion, the complexity of the image data is reduced, enabling a focused analysis of the image structures. The decision of whether noise reduction should be applied and which specific method to use largely depends on the initial image quality and the requirements for the accuracy of Poraver particle detection. If image processing does not deliver the desired accuracy in identifying Poraver particles, reviewing and, if necessary, adjusting noise reduction techniques provide an important approach to improving image quality. The decision of whether to use noise reduction methods and which methods to employ depends heavily on the image situation, which is assessed through visual inspection. It is important to ensure consistency in the assessment process.

4.3.2 Image Segmentation

After converting the grinding images to grayscale, the next step is to segment the Poraver particles from the background. Segmentation is crucial for isolating specific features or areas within the image for further analysis. This chapter focuses on two essential segmentation techniques—the thresholding method using Otsu's method and the global thresholding method—as well as the application of morphological operations to enhance segmentation results.

The application of a thresholding method, described in section 2.6.3, is an effective approach to separate the Poraver particles from the background (the red adhesive). Since the particles are white and the cement paste is red, this method is able to find an intensity value that effectively separates the two materials. Of the three thresholding methods described in section 2.6.3, a combination of Otsu's method and the global thresholding method is chosen. This innovative combination achieves an optimal balance between automation and user control. It provides an automatic, user-friendly approach while also allowing flexibility in situations where manual adjustments are required. As described in section 2.6.3, Otsu's method automatically determines a threshold by analyzing the image histograms (Figure 4-11), which maximizes the variance between classes (foreground and background). In this histogram, the vertical axis represents the number of pixels in the image, while the horizontal axis represents the threshold value of the pixels. Thus, this histogram provides an overview of the distribution of threshold values in the image. Red lines indicate the optimal threshold value calculated by Otsu's method for the image. Otsu's method is particularly well-suited for images with a clear contrast between objects and the background. Due to its automatic threshold determination, it is user-friendly and provides consistent results across different images.

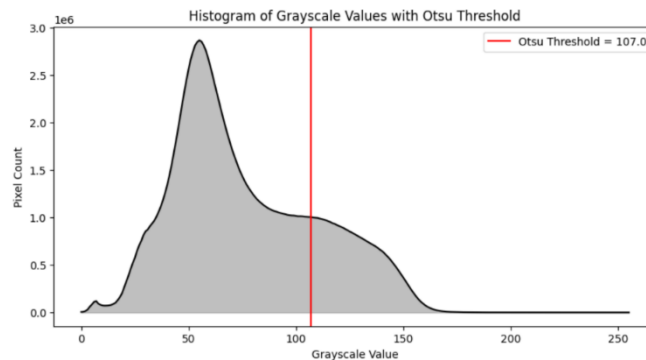


Figure 4-11: Histogram of the image analyzed by Otsu's method and Otsu's threshold

Despite the efficiency of automatic threshold determination, certain image conditions or specific analysis requirements may necessitate manual adjustments. The global thresholding method allows for manual refinement of the threshold calculated by Otsu's method to meet specific segmentation needs. Implementing this method (Appendix A) begins with displaying the histogram of the threshold distribution in the cross-sectional image (Figure 4-11). This histogram visualizes the intensity distribution of pixels and serves as the basis for determining the optimal threshold through Otsu's method. Subsequently, the optimal threshold determined by Otsu's method is shown (Figure 4-11). This automatically determined threshold serves as an effective starting point for segmentation and as a reference point for manual adjustment. Based on this, users can fine-tune the threshold to optimize segmentation results. Figure 4-12 shows cross-sectional images processed by Otsu's threshold and by global threshold with a manual input of 90. This approach allows for more precise control over segmentation. The global thresholding method serves as an additional procedure, offering fine calibration in case the results of Otsu's method are unsatisfactory.

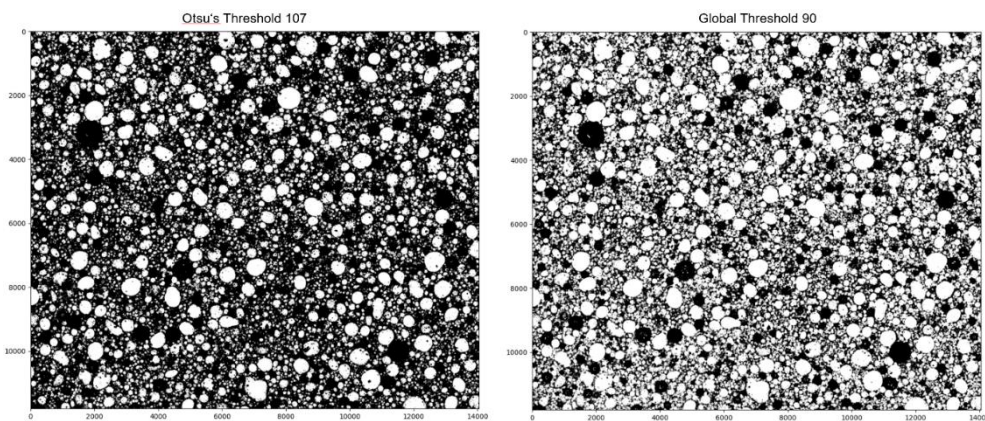


Figure 4-12: Comparison between Otsu's Threshold and Global Threshold with manual input

After applying a thresholding method, morphological operations are used as needed to further refine the segmentation results. These operations, detailed in section 2.6.4, such as opening (erosion followed by dilation) and closing (dilation followed by erosion), are aimed at removing noise, closing gaps, and defining object contours more clearly. Opening effectively reduces small noise and separates loosely connected objects, resulting in a clearer representation. Closing helps to fill in small gaps within objects and connect interrupted contours, preserving object shapes better (Figure 4-13). The combination of these techniques allows for precise segmentation of the image contents and forms the basis for subsequent analysis of homogeneity and other relevant features.

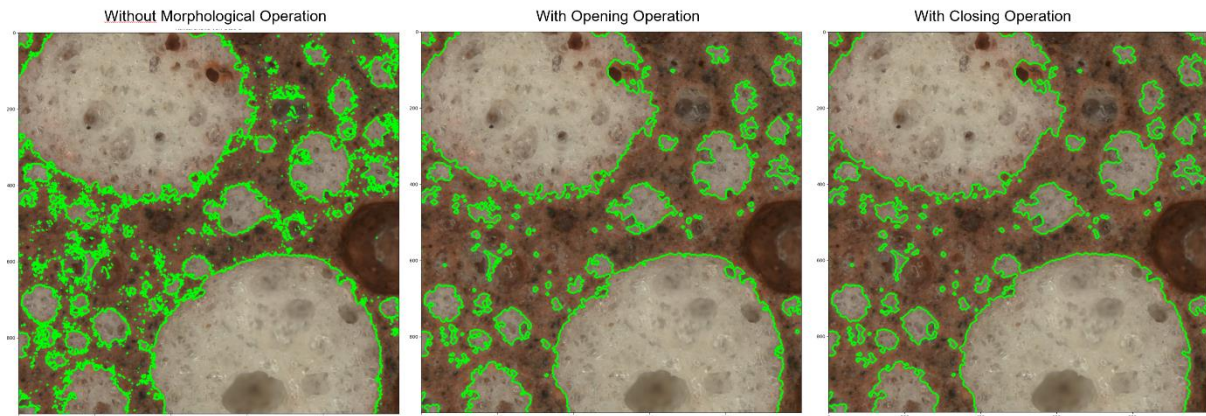


Figure 4-13: Comparison between the use of different morphological operations

4.3.3 Image Processing Validation

Image Processing Validation is a crucial step to ensure that the processing steps performed yield reliable and meaningful results for analysis. This chapter deals with the methods and criteria for evaluating the effectiveness of image processing and the suitability of the processed images for subsequent statistical analysis.

The validation of image processing in the context of statistical analysis in section 4.4 focuses on determining the areas occupied by Poraver particles within the entire corresponding cross-sectional image. The aim is to verify whether the area fractions obtained through image processing represent a realistic depiction of the actual Poraver distribution. A direct but labor-intensive method would involve manually counting and measuring each Poraver particle to determine its exact area fraction and comparing these values with the results of image analysis. Given the high effort and limitations of manual methodology, this work pursues a more efficient approach.

By applying the script developed in section 4.4 (Appendix A), the processed cross-sectional images are divided into uniform, resizable sections. For each of these sections, the identified Poraver particles are projected onto the original image to generate a visually verifiable contour of each particle. This method allows for precise calculation of the Poraver fraction for each image section and provides the opportunity for visual inspection by comparing the sections. Figure 4-14 displays four randomly selected sections out of a total of 63 areas. These sections enable the evaluation of the results of the image processing methods through visual inspection.

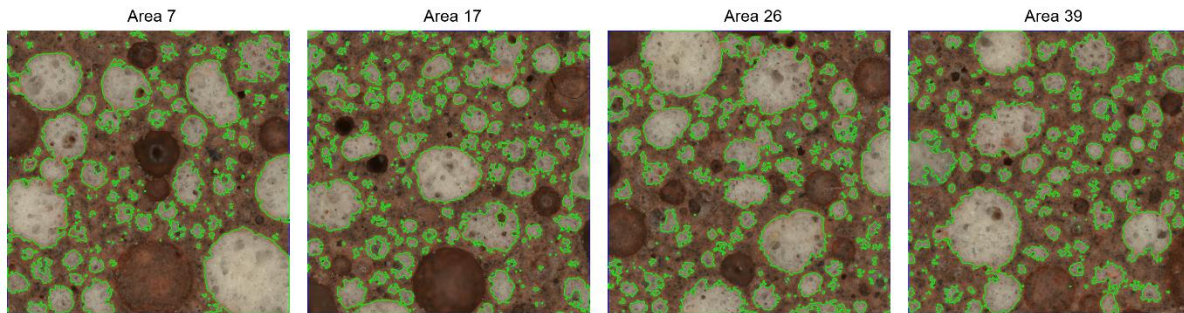


Figure 4-14: Customized image processing method for validation

The flexibility of this image processing method allows for adjustments and optimizations to enhance the accuracy of the analysis without necessitating perfect alignment. Consistency in method and settings across all samples is crucial to ensure a comparable basis for analysis. Uniformity in sample preparation and image processing minimizes variances and enables a focused examination of trends within material homogeneity. This approach balances potential tolerances arising from sample preparation and image processing in comparisons. It ensures that the focus lies not on absolute accuracy but on the consistency of procedures and the discernible trend in material distribution and quality.

4.4 Statistical Analysis

This section describes in detail the implementation of the statistical analysis of mortar mix homogeneity. Using STD and CV (Section 2.4.3) as key indicators, a systematic and standardized method for evaluating mixing quality is presented. These statistical tools enable precise quantification of homogeneity and variability in the mortar mixes produced with the GRES V1.3 system. Through this analysis, conclusions can be drawn regarding the consistency and reliability of the mixing process, ultimately identifying the efficiency and optimization potential of the NNM system.

4.4.1 Implementation of Statistical Analysis of Area Fractions

The aim of the homogeneity analysis is to evaluate the extent of Poraver distribution within the mortar, thereby assessing the mixing quality of the GRES mixing area. To ensure the evaluation yields sophisticated results, it is desirable to analyze as many samples as possible and compare them with each other. The basic idea of the analysis is to enable the comparison of area fractions both within a single micrograph and between multiple micrographs.

The comparison of area fractions is carried out by calculating three measures: mean, STD and CV. These values are suitable for comparison within individual micrographs as well as between multiple micrographs, as long as the comparison areas are identical. To better understand the calculation, the three statistical measures are first introduced computationally. The mean, also known as the average, is a fundamental concept in statistics that describes the central tendency of a set of data. It is calculated by dividing the sum of all Poraver area fractions in the area group by the number of areas. [Mat-2023] Mathematically, the mean (μ) of a group of area fractions x_1, x_2, \dots, x_n in [%] is calculated using the following formula:

$$\mu = \frac{1}{n} \sum_{i=1}^n x_i \text{ [%]} \quad (4-1)$$

where μ is the mean of the area group, n is the number of areas in the area group, and x_i is each individual area fraction in the area group. In the homogeneity analysis, the mean is used to describe the average distribution of the area fraction of Poraver particles across different areas or groups of micrographs. A high mean could indicate an overall dense distribution of particles, while the deviation of individual values from the mean (assessed by the STD and CV) provides insights into the uniformity of this distribution.

The STD is a statistical measure that describes the spread or variability of a set of area fractions around their mean. It indicates how far the individual area fractions are, on average, from the mean of the total area fractions. A low STD means that the area fractions are tightly grouped around the mean, while a high STD indicates that the area fractions are spread over a wider range. For an area collection x_1, x_2, \dots, x_n with mean μ , the STD (σ) is calculated as follows:

$$\sigma = \sqrt{\frac{1}{n} \sum_{i=1}^n (x_i - \mu)^2} \quad (4-2)$$

Where n is the number of areas, x_i represents each individual area fraction, and μ is the mean of the area fractions. In the homogeneity analysis of mortar samples, the STD of the area fractions of Poraver particles indicates how uniformly these materials are distributed within a micrograph or across multiple cross-sectional image within a sample or across multiple samples. A low STD in the area group would suggest a uniform distribution of particles, often indicative of good material homogeneity.

Conversely, a high standard deviation would indicate an uneven distribution, potentially signaling issues in material mixing or processing.

The coefficient of variation (CV) is a statistical measure that expresses the relative variability or dispersion of the area group in relation to its mean. It is typically expressed as a percentage and provides a standardized way to compare the dispersion of area fractions even when the means vary widely. The CV is particularly useful in situations where the units of measurement of the data or the magnitudes of the means differ, as it is a dimensionless number. The CV is calculated by the formula:

$$CV = \left(\frac{\sigma}{\mu} \right) \times 100\% \quad (4-3)$$

Where σ is the STD of the area group, μ is the mean of the area group (assuming μ is not zero). A high CV indicates a large variability relative to the mean, which may suggest a wide dispersion of area fractions around the mean. A low CV suggests that the data are relatively homogeneous and that the dispersion relative to the mean is small. The main advantage of the CV is that it allows for comparing the variability of area fractions measured on different scales or in different units.

Moreover, the CV value is an optimal metric for assessing the homogeneity of the compared areas. To determine the CV value, the areas being compared must first be divided into uniform, identical areas. This step is necessary to ensure that the scope of analysis remains consistent. The unit of distribution should correspond to reality (e.g., in mm), even though the Poraver fraction calculations are performed in pixels in Python. Therefore, scales of pixels/mm should be documented and adjusted (details in Appendix A). The advantage is that during micrograph processing and acquisition, there is more flexibility to compromise on device properties. For the sample generated through the experiment in section 4.1.1 and placed in the 3-gang Mortar Prism Mould for drying and shaping, which have a cross-section of 40 x 40 mm and Poraver particles ranging from 0.1 mm to 2 mm in size, a fixed grid area of 4mm x 4mm as a unit area in a cross-sectional image is meaningful. This unit area allows for a sufficient number of particles in each unit area to draw statistically significant conclusions about the distribution and make the results comparable between different micrographs (Figure 4-15).



Figure 4-15: The micrograph is segmented into defined area units, and the Poraver content is calculated for each respective area unit.

Poraver fraction is individually calculated for each divided area unit, and these values are the values of x_1, x_2, \dots, x_n to be plugged into formulas (4-1), (4-2), and (4-3) to find the CV value for the corresponding areas.

Low CV, also referred to as low variability, are CV values between 0% and 20%. Where 0% to 10% is often considered as very good homogeneity. The data points are very close to the mean, indicating a very uniform distribution or consistency. CV values between 10% and 20% can still be considered as good homogeneity, especially in applications where minor variations are acceptable. CV values between 20% and 30% are classified as moderate CV and may be termed as moderate variability. Depending on the context, this may be acceptable, but it could also suggest that improvements in

processes or controls are needed to reduce variability. High CV, also known as high variability, are CV values above 30%. These are often considered as indicators of high inhomogeneity. This may suggest issues in the manufacturing process, material quality, or sampling and may require further investigations or adjustments to improve homogeneity.

However, this general guideline is only suitable for a rough estimation. It is impossible and unnecessary to set an exact target CV value. As a mixing quality testing method, it is sensible to check the changes in CV values during the mixing process. If the CV value drops from high to low during the mixing process and then fluctuates only within the low CV range, it is a clear indication that at that point, the CV value no longer changes significantly, indicating that the materials are adequately mixed or that the mixing area's limit has been reached, and further improvement is not possible.

4.4.2 Validation of the Statistical Analysis

Now the question arises whether the designed CV value analysis truly reflects the changes in homogeneity. Therefore, it is necessary to validate the CV value analysis. The validation of CV values is crucial to ensure the reliability and accuracy of the results.

A carefully designed validation strategy helps strengthen the credibility of the analysis and ensures that conclusions about the homogeneity of the samples are well-founded. To confirm the accuracy of the methodology, calibrated samples with defined homogeneity properties are used. Comparing the determined CV values with the expected values of these standards can confirm the accuracy of the methodology. The calibrated samples consist of digital pseudo-slice images with near-perfect accuracy of image processing, so that the tolerance of image processing does not obscure the validation with real slice images. To verify the reproducibility of the CV values, the analysis is performed multiple times on the same sample. Low variations in repeated measurements indicate high reliability of the analysis.

The pseudo-slice images consist of red (255, 0, 0) for adhesive and white (0, 0, 0) for Poraver particles. All Poraver particles are circular with a radius of 0.25 mm. The total area is 20 x 20 mm and is divided into 4 equal areas. Four cases covering low, medium, and high CV ranges will be examined. In these 4 cases, homogeneity analysis will be performed multiple times each. First, the pseudo-slice images will be processed with the same image processing method. Thus, even if small tolerances arise from image processing, the sources of tolerance remain identical. This still makes processed images comparably good. Then, the global Poraver proportion will be examined. The

expected Poraver proportion is calculated as follows, where $P_{Poraver_total}\%$ corresponds to the global Poraver proportion, $A_{Poraver_total}$ corresponds to the total Poraver area, A_{total} corresponds to the total slice image area, and $N_{Poraver_total}$ corresponds to the total Poraver count:

$$P_{Poraver_total}\% = \left(\frac{A_{Poraver_total}}{A_{total}} \right) \times 100\% \quad (4-4)$$

$$= \left(\frac{N_{Poraver_total} \times A_{Poraver_particle}}{A_{total}} \right) \times 100\% \quad (4-5)$$

Since we already know that pseudo-images are designed as 20 x 20 mm areas, and all Poraver particles are circular with a diameter of 0.25 mm, we can calculate the expected Poraver proportion as follows, based on the total number of Poraver particles.

$$P_{Poraver}\% = \left(\frac{N_{Poraver_total} \times \pi \times 0.25^2}{20 \times 20} \right) \times 100 \quad (4-6)$$

The comparison between the expected global Poraver proportion and the calculated global Poraver proportion will verify the accuracy of the image processing. All 4 cases will contain exactly 400 Poraver particles, resulting in a global Poraver proportion of 19.63%. Next, the pseudo-images will be divided into 4 regions, each with a size of 10 x 10 mm as the area unit. The Poraver proportion will be calculated for each area unit, and these values will be used to calculate the CV for all 4 regions, thereby determining the assessment of homogeneity of the pseudo-images.

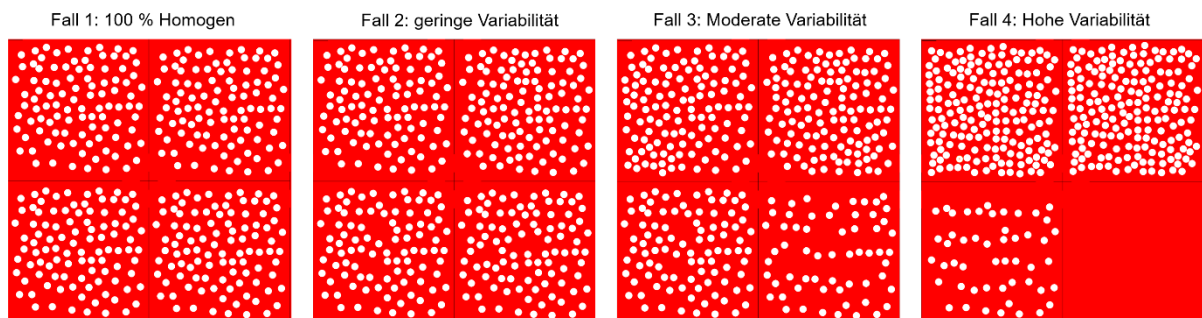


Figure 4-16: Pseudo-slice images with 4 extreme cases

As shown in Figure 4-16, the 4 cases are distributed by area as shown in Table 4-4. The expected and calculated CV values from the designed system can be seen in Table 4-5, and the complete analysis data is available in Appendix B. As seen in Figure 4-16, Case 1 shows perfectly distributed Poraver in all areas, Case 2 exhibits slight

differences that could correspond to reality. Cases 3 and 4 represent significantly inhomogeneous scenarios, indicative of poor mixing quality. By comparing the expected results with the calculated ones, the tolerances range from 0.12% to 2.04%, demonstrating good outcomes. Therefore, the designed model could be validated, indicating that the calculated CV values provide a realistic homogeneity analysis.

Table 4-4: *Distribution of the Poraver particles with an identical radius of 0.25 mm with a scale of 85 pixels/mm*

Area Unit	1 [Pcs.]	2 [Pcs.]	3 [Pcs.]	4 [Pcs.]
Fall 1	100	100	100	100
Fall 2	100	109	95	96
Fall 3	120	125	95	60
Fall 4	175	175	50	0

Table 4-5: *Comparison between expected CV and calculated CV in 4 extreme cases*

	Fall 1	Fall 2	Fall 3	Fall 4
Expected CV [%]	0	5.52	25.74	77.06
Calculated CV [%]	0.37	5.41	25.77	77.17

4.5 Interpretation of the Results

In this section, the results of the conducted homogeneity analysis are interpreted, with a specific focus on evaluating the mixing quality of the GRES V1.3 based on samples taken during the experiments. The aim is to gain a comprehensive understanding of the performance and quality of the mixing area and to assess to what extent the GRES V1.3 system can deliver homogeneous material mixes for the NNM process.

Overall, a 43.5 cm long sample was directly extracted from the mixing area, starting at the 16 cm position. This sample was divided into eight pieces, each with a width of 5 cm, resulting in eight cross-sectional images. Additionally, ten samples were taken from the end product of four different experiments and placed in 3-Gang Prism Moulds for drying, resulting in another ten microsections. All extracted samples have a volume ratio of 2.0 between Poraver and adhesive, with the pump speed set at 38.31 Hz and the mixer motor speed at 90.44 rpm. All samples were cut and treated with a color enhancer. Microsections were captured using a microscope at a magnification of x80. Image processing involved conversion to grayscale, application of Otsu's method, and morphological operations with opening followed by closing. The size of the area unit was 4 mm x 4 mm. The analysis results are presented in the table.

Table 4-6: Analysis results of the sample directly from the mixing area

Position	Number of area units	Poraver fraction [%]	Mean value [%]	STD	CV [%]
1	14	30.45	30.39	5.97	19.64
2	78	32.70	32.60	5.91	18.13
3	120	31.10	30.98	5.26	16.98
4	112	37.75	37.62	6.48	17.23
5	90	29.85	29.75	5.13	17.24
6	98	38.60	38.46	6.89	17.92
7	120	15.85	33.15	5.25	15.85
8	77	13.63	33.39	4.55	13.63

Table 4-7: Analysis results of the sample from the end product

Trial No.	Sample No.	Number of area units	Poraver fraction [%]	Mean value [%]	STD	CV [%]
1	1	81	33.85	33.78	5.02	14.86
1	2	64	31.11	31.05	5.26	16.95
2	3	72	36.66	36.56	5.66	15.47
2	4	72	34.48	34.39	6.01	17.48
3	5	72	31.11	31.01	5.21	16.80
3	6	72	33.96	33.87	6.34	18.71
3	7	63	36.47	36.37	7.13	19.62
3	8	72	38.93	38.81	6.78	17.46
4	9	63	34.46	34.37	4.87	14.17
4	10	63	37.18	37.08	4.80	12.94

The analysis of the results from the samples taken directly from the mixing area as well as the samples from the end product indicates homogeneity with CV values all falling within the range of 10% to 20%. These values suggest that the mixtures can be classified as homogeneous; however, they do not indicate optimal homogeneity. Contrary to the expectation that samples from the mixing area should show a trend of high to lower CV values, indicating increasing homogeneity along the mixing area, this trend is absent. It is likely that homogeneity has already stabilized before the 16 cm mark of the mixing area, and from this position onward, the mixing quality is already acceptable. Nonetheless, samples from positions 1 to 8 show a slight improvement in homogeneity.

However, to make more precise statements, additional experiments and sample analyses are necessary. This would allow for a more detailed assessment of homogeneity development along the entire mixing area and understanding whether and how homogeneity improves with increasing distance from the beginning of the mixing process. While the current results provide valuable insights, they also indicate the need for further research to comprehensively optimize and evaluate mixing quality in the NNM system with GRES V1.3.

5 Summary

This study focused on systematically classifying Near-Nozzle Mixing (NNM) and analyzing the homogeneity of mortar mixtures produced by the innovative NNM System GRES V1.3. The goal was to optimize mixing quality for developing reproducible, high-quality, and 3D-printable mortar suitable for additive manufacturing in construction. Extensive experimental series were conducted, systematically adjusting formulations for adhesive and lightweight mortar (LWM) to meet printability, structural integrity, and durability requirements.

A significant contribution of this study is the systematic classification and detailed analysis of NNM technology. The NNM process was classified under E3DCP and further categorized at the processing system level under the 2K system, demonstrating the potential of NNM in both single-material and multi-material additive manufacturing. This systematic approach facilitates the classification of NNM processes in additive manufacturing for construction, highlighting its role in the field.

The homogeneity analysis methodology involved systematically sampling specimens from various areas of the mixing system, processing them, and acquiring micrographs. Advanced image processing techniques, combined with extensive statistical analysis using standard deviation (STD) and coefficient of variation (CV), enabled precise evaluation of mortar mixture homogeneity through Poraver area fraction in cross-section images. The results confirm the GRES V1.3 system's capability to produce uniform and homogeneous mortar mixtures that meet the stringent requirements of 3D printing in construction.

6 Limitations and Outlook

In the present study, progress has been made in the classification and homogeneity analysis for evaluating the mixing quality of the Near-Nozzle Mixing (NNM) System GRES V1.3. The successful application of specific methods for assessing and improving the homogeneity of mortar mixtures forms a solid foundation for future research endeavors. The following are potential directions for further studies that have the potential to further revolutionize additive manufacturing in construction:

The study has some limitations that should be acknowledged. One limitation concerns the chemical properties analysis, which couldn't be made in this study. Due to the nature of the sampling method, there is a risk that the sample retrieved may not accurately represent the chemical composition of the entire mixing area. This could lead to inaccuracies in the assessment of the material properties and potentially affect the overall conclusions drawn from the study. Another limitation is related to the sampling depth. The sampling depth is limited to the first 16 cm of the mixing zone, which may not fully capture the entire distribution of materials within the zone. This limitation could impact the accuracy of the homogeneity analysis and may result in the loss of valuable data.

Despite these limitations, there are several promising avenues for future research. One potential direction is the development of advanced sampling techniques that can provide more representative samples of the mixing area. This could involve the use of robotic sampling devices or automated sampling procedures to ensure thorough coverage of the entire mixing area. Another area for future research is the integration of real-time monitoring systems to continuously assess mixing quality during the printing process. This could help identify any deviations or inconsistencies in real-time and enable prompt adjustments to optimize mixing performance. Additionally, further investigation into the influence of printing parameters on mixing quality could help refine printing processes and improve overall print quality. Overall, by addressing these challenges and exploring new opportunities, future research has the potential to further advance additive manufacturing in construction and pave the way for the development of innovative and sustainable building solutions.

Bibliography

- [Abd-2019] Abdulhameed, O.; Al-Ahmari, A.; Ameen, W.; Mian, S. H.: Additive manufacturing: Challenges, trends, and applications. In: *Advances in Mechanical Engineering*, Jg. 11 (2019) Nr. 2, S. 168781401882288.
- [Add-2024a] Additive Manufacturing in Construction AMC TRR 277: AMC TRR277 PROJECT A03. <https://amc-trr277.de/projects/project-area-a/focus-area-project-a03/>, Aufruf am
- [Add-2024b] Additive Manufacturing in Construction AMC TRR 277: AMC TRR277 Research. <https://amc-trr277.de/>, Aufruf am
- [Alt-2022] Altıparmak, S. C.; Yardley, V. A.; Shi, Z.; Lin, J.: Extrusion-based additive manufacturing technologies: State of the art and future perspectives. In: *Journal of Manufacturing Processes*, Jg. 83 (2022), S. 607–636.
- [Bou-2020] Bourell, D. L.; Frazier, W.; Kuhn, H.; Seifi, M.: *Additive Manufacturing Processes*. ASM International, 2020.
- [Bro-1991] Brown, D.; Heaton, B. T.; Iggo, J. A.: Applications of Spectroscopic Measurements to Homogeneous Catalysis. In: Ugo, R., et al. (Hrsg.): *Metal Promoted Selectivity in Organic Synthesis*. Springer Netherlands, Dordrecht, 1991, S. 329–365.
- [Bun-2016] Bunoïu, R.; Ramdani, K.: Homogenization of materials with sign changing coefficients. In: *Communications in Mathematical Sciences*, Jg. 14 (2016) Nr. 4, S. 1137–1154.
- [Bus-2020] Buswell, R. A.; Da Silva, W. L.; Bos, F. P.; Schipper, H. R.; Lowke, D.; Hack, N.; Kloft, H.; Mechtcherine, V.; Wangler, T.; Roussel, N.: A process classification framework for defining and describing Digital Fabrication with Concrete. In: *Cement and Concrete Research*, Jg. 134 (2020), S. 106068.
- [Che-2023] Chen, H.; Zhang, D.; Chen, P.; Li, N.; Perrot, A.: A Review of the Extruder System Design for Large-Scale Extrusion-Based 3D Concrete Printing. In: *Materials (Basel, Switzerland)*, Jg. 16 (2023) Nr. 7
- [Chr-2023] Christian Maximilian Hechtel, M. Sc.; Thomas Kränkel, D.-I.; Christoph Gehlen: Near-Nozzle Mixing for Additive Manufacturing of

Cementitious Mortar: A Homogeneity Study. In: *ce papers*, Jg. 2023 (2023) Nr. 6, S. 812–817.

- [Del-2018] Delgado Camacho, D.; Clayton, P.; O'Brien, W. J.; Seepersad, C.; Juenger, M.; Ferron, R.; Salamone, S.: Applications of additive manufacturing in the construction industry – A forward-looking review. In: *Automation in Construction*, Jg. 89 (2018), S. 110–119.
- [Gos-2016] Gosselin, C.; Duballet, R.; Roux, P.; Gaudillière, N.; Dirrenberger, J.; Morel, P.: Large-scale 3D printing of ultra-high performance concrete – a new processing route for architects and builders. In: *Materials & Design*, Jg. 100 (2016), S. 102–109.
- [Ham-2019] Hamidi, F.; Aslani, F.: Additive manufacturing of cementitious composites: Materials, methods, potentials, and challenges. In: *Construction and Building Materials*, Jg. 218 (2019), S. 582–609.
- [Hei-2022] Heidarneshad, F.; Zhang, Q.: Shotcrete based 3D concrete printing: State of art, challenges, and opportunities. In: *Construction and Building Materials*, Jg. 323 (2022), S. 126545.
- [Hil-2021] Hillmann, S.; Köhler, B.: Inspection of Ceramic Materials. In: Meyendorf, N., et al. (Hrsg.): *Handbook of Nondestructive Evaluation 4.0*. Springer International Publishing, Cham, 2021, S. 1–20.
- [ISO-52900] ISO International Organization for Standardization; ASTM: Additive manufacturing — General principles — Terminology. ISO/ASTM Nr. 52900, 2015.
- [Jia-2023] Jiayi An: Mixing Quality evaluation of a Near-Nozzle-Mixing (NNM) Process - Validation, DEM-Simulation and Model Evaluation. Master's Thesis. Chair of Materials Handling, Material Flow, Logistics, Technical University of Munich, Arcisstraße 21, 80333 München, 2023.
- [Jup-2024] Jupyter Trademark: About Us - Project Jupyter's origins and governance, Aufruf am
- [Kru-2019] Kruger, J.; Zeranka, S.; van Zijl, G.: An ab initio approach for thixotropy characterisation of (nanoparticle-infused) 3D printable concrete. In: *Construction and Building Materials*, Jg. 224 (2019), S. 372–386.

- [Lim-2012] Lim, S.; Buswell, R. A.; Le, T. T.; Austin, S. A.; Gibb, A.; Thorpe, T.: Developments in construction-scale additive manufacturing processes. In: *Automation in Construction*, Jg. 21 (2012), S. 262–268.
- [Lou-2023] Loughborough University: Revolutionising the construction industry. <https://www.lboro.ac.uk/departments/abce/working-with-business/impact/3d-concrete-printing/>, Aufruf am
- [Low-2018] Lowke, D.; Dini, E.; Perrot, A.; Weger, D.; Gehlen, C.; Dillenburger, B.: Particle-bed 3D printing in concrete construction – Possibilities and challenges. In: *Cement and Concrete Research*, Jg. 112 (2018), S. 50–65.
- [Lu-2020] Lu, B.; Zhu, W.; Weng, Y.; Liu, Z.; Yang, E.-H.; Leong, K. F.; Tan, M. J.; Wong, T. N.; Qian, S.: Study of MgO-activated slag as a cement-less material for sustainable spray-based 3D printing. In: *Journal of Cleaner Production*, Jg. 258 (2020), S. 120671.
- [Mat-2023] Matuszek, D. B.; Biłos, Ł. A.; Królczyk, J. B.: Image Analysis in the Assessment of Homogeneity of Fine-Grained Mixtures. In: Pascuzzi, S.; Santoro, F. (Hrsg.): *Farm Machinery and Processes Management in Sustainable Agriculture*. Springer International Publishing, Cham, 2023, S. 179–190.
- [Mec-2020] Mechtcherine, V.; Bos, F. P.; Perrot, A.; Da Silva, W. L.; Nerella, V. N.; Fataei, S.; Wolfs, R.; Sonebi, M.; Roussel, N.: Extrusion-based additive manufacturing with cement-based materials – Production steps, processes, and their underlying physics: A review. In: *Cement and Concrete Research*, Jg. 132 (2020), S. 106037.
- [Mic-2016] Michael Molitch-Hou: Dubai Unveils First 3D-Printed Office Building – The Office of the Future is first building 3D printed as part of Dubai 3D Printing Strategy. <https://www.engineering.com/story/dubai-unveils-first-3d-printed-office-building>, Aufruf am
- [Moh-2021] Mohan, M. K.; Rahul, A. V.; Schutter, G. de; van Tittelboom, K.: Extrusion-based concrete 3D printing from a material perspective: A state-of-the-art review. In: *Cement and Concrete Composites*, Jg. 115 (2021), S. 103855.

- [Mon-2021] Monaldo, E.; Marfia, S.: Multiscale technique for the analysis of 3D-printed materials. In: International Journal of Solids and Structures, Jg. 232 (2021), S. 111173.
- [Pac-2021] Pacillo, G. A.; Ranocchiai, G.; Loccarini, F.; Fagone, M.: Additive manufacturing in construction: A review on technologies, processes, materials, and their applications of 3D and 4D printing. In: Material Design & Processing Communications, Jg. 3 (2021) Nr. 5
- [Paj-2022] Pajonk, A.; Prieto, A.; Blum, U.; Knaack, U.: Multi-material additive manufacturing in architecture and construction: A review. In: Journal of Building Engineering, Jg. 45 (2022), S. 103603.
- [Pao-2019] Paolini, A.; Kollmannsberger, S.; Rank, E.: Additive manufacturing in construction: A review on processes, applications, and digital planning methods. In: Additive Manufacturing, Jg. 30 (2019), S. 100894.
- [Pei-2023] Pei, E.; Bernard, A.; Gu, D.; Klahn, C.; Monzón, M.; Petersen, M.; Sun, T.: Springer Handbook of Additive Manufacturing. Springer International Publishing, Cham, 2023.
- [Por-2024] Poraver GmbH: Poraver expanded glass. <https://poraver.com/>, Aufruf am
- [Pyt-2024a] Python Software Foundation: Newest success stories. <https://www.python.org/success-stories/>, Aufruf am
- [Pyt-2024b] Python Software Foundation: The Python Wiki. <https://wiki.python.org/moin/>, Aufruf am
- [Ros-2013] Rosas, J. G.; Armenta, S.; Cruz, J.; Blanco, M.: A new approach to determine the homogeneity in hyperspectral imaging considering the particle size. In: Analytica chimica acta, Jg. 787 (2013), S. 173–180.
- [Ruf-2022] Ruffray, N.; Reiter, L.; Flatt, R. J.: Overcoming Environmental Stress Cracking of FDM 3D Printed Formwork for Counter-Pressure Casting of Concrete. In: 3D printing and additive manufacturing, Jg. 9 (2022) Nr. 2, S. 122–131.
- [Sab-2002] Sabliov, C. M.; Boldor, D.; Keener, K. M.; Farkas, B. E.: IMAGE PROCESSING METHOD TO DETERMINE SURFACE AREA AND VOLUME OF AXI-SYMMETRIC AGRICULTURAL PRODUCTS.

In: International Journal of Food Properties, Jg. 5 (2002) Nr. 3, S. 641–653.

- [Sal-2018] Salet, T. A. M.; Ahmed, Z. Y.; Bos, F. P.; Laagland, H. L. M.: Design of a 3D printed concrete bridge by testing. In: Virtual and Physical Prototyping, Jg. 13 (2018) Nr. 3, S. 222–236.
- [Sar-2010] Saravanan, C.: Color Image to Grayscale Image Conversion 2010 Second International Conference on Computer Engineering and Applications, 2010, S. 196–199.
- [Sch-2018] Schutter, G. de; Lesage, K.; Mechtcherine, V.; Nerella, V. N.; Habert, G.; Agusti-Juan, I.: Vision of 3D printing with concrete — Technical, economic and environmental potentials. In: Cement and Concrete Research, Jg. 112 (2018), S. 25–36.
- [See-2023] Seelaboyina, R.; Vishwakarma, R.: Different Thresholding Techniques in Image Processing : A Review. In: Kumar, A.; Senatore, S.; Gunjan, V. K. (Hrsg.): ICDSMLA 2021. Springer Nature Singapore, Singapore, 2023, S. 23–29.
- [Sid-2020] Siddika, A.; Mamun, M. A. A.; Ferdous, W.; Saha, A. K.; Alyousef, R.: 3D-printed concrete: applications, performance, and challenges. In: Journal of Sustainable Cement-Based Materials, Jg. 9 (2020) Nr. 3, S. 127–164.
- [Soi-2004] Soille, P.: Morphological Image Analysis. Springer Berlin Heidelberg, Berlin, Heidelberg, 2004.
- [Tan-2022] Tan, Y.; Dahlenburg, M.; Fottner, J.; Kessler, S.: Influencing factors of the mixing performance of a near-nozzle continuous mixer for 3D concrete printing: An analysis based on spatial Lacey mixing index (SLMI). In: Powder Technology, Jg. 403 (2022), S. 117414.
- [Wan-2022] Wangler, T.; Pileggi, R.; Gürel, S.; Flatt, R. J.: A chemical process engineering look at digital concrete processes: critical step design, inline mixing, and scaleup. In: Cement and Concrete Research, Jg. 155 (2022), S. 106782.
- [Yuc-2019] Yucel, A. O.; Guler, M.: Characterization of Homogeneity of Asphalt Concrete Using 2D Cross-Sectional Images. In: Pradhan, B. (Hrsg.): GCEC 2017. Springer Singapore, Singapore, 2019, S. 273–281.

List of Figures

Figure 2-1:	Classification of manufacturing processes [Abd-2019]	4
Figure 2-2:	Classification of AM processes depending on the state of raw material [Abd-2019]	5
Figure 2-3:	Left: Curved bench constructed by Loughborough University [Lou-2023]. Right: Office building constructed by WinSun [Mic-2016].	7
Figure 2-4:	Process classification [Bus-2020]	8
Figure 2-5:	Process classification of particle-bed methods [Bus-2020]	8
Figure 2-6:	Schematic figure of particle-bed 3D printing techniques in construction [Low-2018]	9
Figure 2-7:	The RILEM process classification framework for DFC technologies [Bus-2020]	11
Figure 2-8:	Illustration of various processing steps in concrete extrusion 3D printing processes. 1K do not include the secondary mixing step of an accelerator just before extrusion, as in the 2K systems. [Wan-2022]	13
Figure 2-9:	Left: SC3DP with substrate/reinforcement [Hei-2022]; Right: Free-formed SC3DP [Lu-2020]	14
Figure 2-10:	Categorization tree for MMAM Processes in Architecture and Construction [Paj-2022]	16
Figure 2-11:	CAD Modell of GRES V1.3	20
Figure 3-1:	Process classification of NNM process	33
Figure 4-1:	Cross-section of the current prototype GRES V1.3, Credit_ Maximilian Dahlenburg, TUM	36
Figure 4-2:	Rendering of GRES V1.3 in periphery, Credit cbm, fml TUM, P. Schneider	41
Figure 4-3:	Position of the grid bin for evaluating the mixing performance [Jia-2023]	42

Figure 4-4:	Sample extraction from the mixing zone: 435 mm in length, starting at 160 mm	43
Figure 4-5:	Left: Sample extraction from the end product; Right: Dried and demolded sample.	43
Figure 4-6:	Left: Wet cutting of samples in cubic meters at Centrum Baustoffe und Materialprüfung; top right: Cut samples from the end product; bottom right: Cut samples from the mixing zone.	44
Figure 4-7:	Comparison between untreated and color-enhanced samples.	45
Figure 4-8:	Left: Keyence VHX digital microscope at the Institute for Machine Tools and Industrial Management; right: Captured cross-section image	45
Figure 4-9:	Comparison between original image and grayscale image.	47
Figure 4-10:	Comparison between using different noise reduction methods	48
Figure 4-11:	Histogram of the image analyzed by Otsu's method and Otsu's threshold	49
Figure 4-12:	Comparison between Otsu's Threshold and Global Threshold with manual input	50
Figure 4-13:	Comparison between the use of different morphological operations	51
Figure 4-14:	Customized image processing method for validation	52
Figure 4-15:	The micrograph is segmented into defined area units, and the Poraver content is calculated for each respective area unit.	55
Figure 4-16:	Pseudo-slice images with 4 extreme cases	57

List of Tables

Table 2-1:	Composition of the cement paste [Chr-2023]	21
Table 2-2:	Characteristics of the LWM composition [Chr-2023]	21
Table 2-3:	Material performance for LWM in the fresh and hardened state; measured mean mortar property with the standard deviation (STD) and related coefficient of variation (CV). [Chr-2023]	21
Table 5-1:	Recipe for Poraver mixture	37
Table 4-2:	Basic Recipe for Cement Paste Mixture	38
Table 4-3:	Adapted Recipe for Cement Paste Mixture with Red Pigments	38
Table 5-4:	Distribution of the Poraver particles with an identical radius of 0.25 mm with a scale of 85 pixels/mm	58
Table 5-5:	Comparison between expected CV and calculated CV in 4 extreme cases	58
Table 4-6:	Analysis results of the sample directly from the mixing area	59
Table 5-7:	Analysis results of the sample from the end product	59

A Appendix

The Script of Image Processing

Importing the necessary libraries

Importieren nötige Bibliotheken

```
import cv2
```

```
import numpy as np
```

```
from scipy import ndimage
```

```
import pandas as pd
```

```
import os
```

```
import matplotlib.pyplot as plt
```

Loading the Cross-Sectional Image

- Adding the name of the test image and filling in the appropriate format.
- The image must be in the same folder as the notebook for the program to locate it.

Bild laden

```
original_bild = cv2.imread('20240308_211804_T_21.02.24.tif')
```

Image Preprocessing

Conversion of the Image to Grayscale

Konvertierung in Graustufen

```
graustufen_bild = cv2.cvtColor(original_bild, cv2.COLOR_BGR2GRAY)
```

Noise Reduction (Optional)

Gaussian Blur

```
gaußscher_geglattetes_bild = cv2.GaussianBlur(graustufen_bild, (5, 5), 0)
```

Median-Filter

```
median_geglattetes_bild = cv2.medianBlur(graustufen_bild, 5)
```

Bilateral Filter

```
bilaterales_bild = cv2.bilateralFilter(graustufen_bild, 9, 75, 75)
```

Image Segmentation

Thresholding

Otsu's Method

- Automatic thresholding method

```
# Otsu's Schwellenwert anwenden
```

```
ret, otsu_thresh_bild = cv2.threshold(graustufen_bild, 0, 255, cv2.THRESH_BINARY + cv2.THRESH_OTSU)
```

- Displaying Otsu's threshold

```
# Ausgabe des von Otsu's Methode gefundenen Schwellenwerts
```

```
print(f"Der optimale Schwellenwert ist: {ret}")
```

- Displaying the histogram

```
# Anteigen der Verteilung der Schwellenwerte durch Histogramm der Grauwerte des Bildes
```

```
# Histogramm der Grauwerte berechnen
```

```
histogramm = cv2.calcHist([original_bild], [0], None, [256], [0, 256])
```

```
# Histogramm der Grauwerte anzeigen
```

```
plt.figure(figsize=(10, 5))
```

```
plt.plot(histogramm, color='black')
```

```
plt.fill_between(range(256), histogramm[:, 0], color='gray', alpha=0.5)
```

```
plt.axvline(x=ret, color='red', label=f"Otsu Threshold = {ret}")
```

```
# Achsen und Legende
```

```
plt.xlabel('Grayscale Value')
```

```
plt.ylabel('Pixel Count')
plt.legend()
plt.title('Histogram of Grayscale Values with Otsu Threshold')
plt.show()
```

Global Thresholding

- Suitable for manual threshold setting

Eingabe von globalen Schwellenwert

```
schwellenwert = 90
```

Globales Schwellenwertverfahren anwenden

```
ret, globalschwellenwert_bild = cv2.threshold(graustufen_bild, schwellenwert, 255,
                                             cv2.THRESH_BINARY)
```

Morphological Operation

Erstellen eines strukturierenden Elements (kreisförmiger Kernel)

```
kernel = cv2.getStructuringElement(cv2.MORPH_ELLIPSE, (7, 7))
```

Opening

- Removing small objects or noise that remain after binarization. A circular structuring element might be suitable.

Öffnung (Opening): Erosion gefolgt von Dilatation

```
oeffnung = cv2.morphologyEx(otsu_thresh_bild, cv2.MORPH_OPEN, kernel)
```

Closing

- Closing small gaps within the particles and smoothing the edges.

Schließung (Closing): Dilatation gefolgt von Erosion

```
schliessung = cv2.morphologyEx(oeffnung, cv2.MORPH_CLOSE, kernel)
```

Statistical Homogeneity Analysis

Define Unit of Area for Cropping

Abmessungen des Originalbildes

```
original_hoehe, original_breite = original_bild.shape[:2]
```

Skala und gewünschte Teilungsgröße in mm

```
pixel_pro_mm = 384 # Pixel pro mm
```

```
teilungs_groesse_mm = 4 # Teilungsgröße in mm
```

Umrechnung der Teilungsgröße in Pixel

```
teilungs_groesse_pixel = teilungs_groesse_mm * pixel_pro_mm
```

Berechnung, wie oft die Teilungsgröße in die Originalabmessungen passt

```
anzahl_teilungen_breite = original_breite // teilungs_groesse_pixel
```

```
anzahl_teilungen_hoehe = original_hoehe // teilungs_groesse_pixel
```

Berechnung der neuen Abmessungen, die ein Vielfaches der Teilungsgröße sind

```
neue_breite = anzahl_teilungen_breite * teilungs_groesse_pixel
```

```
neue_hoehe = anzahl_teilungen_hoehe * teilungs_groesse_pixel
```

Bild zuschneiden, um es durch die Teilungsgröße teilbar zu machen

```
geschnittenes_bild = original_bild[:neue_hoehe, :neue_breite]
```

```
print(f"Abmessung von Original Bild: {original_hoehe}*{original_breite} Pixel")
```

```
print(f"Teilungsgröße in Pixel: {teilungs_groesse_pixel}")
```

```
print(f"Wie oft die Teilungsgröße in die Originalabmessungen passt: {anzahl_teilun-  
gen_hoehe}*{anzahl_teilungen_breite}")
```

```
print(f"neue Abmessung: {neue_hoehe}*{neue_breite} Pixel")
```


Implementation of the Selected Image processing Methods and Calculation of the Overall Poraver Content in the Entire Micrograph

In [19]:

```
# Konvertierung in Graustufen
```

```
graustufen_bild = cv2.cvtColor(geschnittenes_bild, cv2.COLOR_BGR2GRAY)
```

```
# Otsu's Schwellenwert anwenden
```

```
ret, otsu_thresh_bild = cv2.threshold(graustufen_bild, 0, 255, cv2.THRESH_BINARY +  
                                     cv2.THRESH_OTSU)
```

```
# Erstellen eines strukturierenden Elements (kreisförmiger Kernel)
```

```
kernel = cv2.getStructuringElement(cv2.MORPH_ELLIPSE, (7, 7))
```

```
# Öffnung (Opening): Erosion gefolgt von Dilatation
```

```
oeffnung = cv2.morphologyEx(otsu_thresh_bild, cv2.MORPH_OPEN, kernel)
```

```
# Schließung (Closing): Dilatation gefolgt von Erosion
```

```
schliessung = cv2.morphologyEx(oeffnung, cv2.MORPH_CLOSE, kernel)
```

```
# Konturen finden
```

```
konturen, _ = cv2.findContours(schliessung, cv2.RETR_EXTERNAL, cv2.CHAIN_APPROX_SIMPLE)
```

```
# Konturen auf das Originalbild zeichnen
```

```
bild_mit_konturen = geschnittenes_bild.copy()
```

```
cv2.drawContours(bild_mit_konturen, konturen, -1, (0, 255, 0), 3)
```

```
# Globale Poraver-Anteil berechnen
```

```
gesamtflaeche_poraver = sum(cv2.contourArea(kontur) for kontur in konturen)
```

```
gesamtflaeche_geschnittenes_bild = geschnittenes_bild.shape[0] * geschnittenes_bild.shape[1]
```

```
poraver_anteil = (gesamtflaeche_poraver / gesamtflaeche_geschnittenes_bild) * 100 # In Pro-  
zent
```

```
print(f"Poraver-Anteil im geschnittenen Bild: {poraver_anteil:.2f}%")
```

Crop the Entire Micrograph into Individual Units based on Area and Calculate the Poraver Content for Each Unit.

```
# Zeichne die Bereichsgrenzen auf das geschnittene bild
```

```
for zeile in range(1, anzahl_teilungen_hoehe):
```

```
    cv2.line(geschnittenes_bild, (0, zeile * teilungs_groesse_pixel), (neue_breite, zeile * tei-  
        lungen_groesse_pixel), (255, 0, 0), 3)
```

```
for spalte in range(1, anzahl_teilungen_breite):
```

```
    cv2.line(geschnittenes_bild, (spalte * teilungs_groesse_pixel, 0), (spalte * teilungs_groesse_pi-  
        xel, neue_hoehe), (255, 0, 0), 3)
```

```
# Liste für die Speicherung der Poraver-Anteile
```

```
poraver_anteile_liste = []
```

```
# Zeichne die Bereichsgrenzen auf das geschnittene bild
```

```
for zeile in range(1, anzahl_teilungen_hoehe):
```

```
    cv2.line(geschnittenes_bild, (0, zeile * teilungs_groesse_pixel), (neue_breite, zeile * tei-  
        lungen_groesse_pixel), (255, 0, 0), 3)
```

```
for spalte in range(1, anzahl_teilungen_breite):
```

```
    cv2.line(geschnittenes_bild, (spalte * teilungs_groesse_pixel, 0), (spalte * teilungs_groesse_pi-  
        xel, neue_hoehe), (255, 0, 0), 3)
```

```
# Liste für die Speicherung der Poraver-Anteile
```

```
poraver_anteile_liste = []
```

```
df_poraver_anteile_liste = []
```

```
# Berechnen und Anzeigen der Poraver-Anteile für jeden Bereich
```

```
fig, axs = plt.subplots(anzahl_teilungen_hoehe, anzahl_teilungen_breite, figsize=(20, 20))
```

```

for zeile in range(anzahl_teilungen_hoehe):
    for spalte in range(anzahl_teilungen_breite):
        bereich = schliessung[zeile * teilungs_groesse_pixel : (zeile + 1) * teilungs_groesse_pixel,
                               spalte * teilungs_groesse_pixel : (spalte + 1) * teilungs_groesse_pixel]

        # Konturen im geschlossenen Bereich finden
        bereich_konturen, _ = cv2.findContours(bereich, cv2.RETR_EXTERNAL, cv2.CHAIN_APPROX_SIMPLE)

        # Konturen auf das Originalbild zeichnen
        bereich_mit_konturen = geschnittenes_bild[zeile * teilungs_groesse_pixel : (zeile + 1) * teilungs_groesse_pixel,
                                                  spalte * teilungs_groesse_pixel : (spalte + 1) * teilungs_groesse_pixel].copy()
        cv2.drawContours(bereich_mit_konturen, bereich_konturen, -1, (0, 255, 0), 3)

        # Berechne den Poraver-Anteil
        gesamtflaeche_bereich = teilungs_groesse_pixel * teilungs_groesse_pixel
        poraver_flaeche_bereich = sum(cv2.contourArea(bereich_kontur) for bereich_kontur in bereich_konturen)
        poraver_anteil_bereich = (poraver_flaeche_bereich / gesamtflaeche_bereich) * 100

        axs[zeile, spalte].imshow(cv2.cvtColor(bereich_mit_konturen, cv2.COLOR_BGR2RGB))
        axs[zeile, spalte].set_title(f"Bereich {zeile * anzahl_teilungen_breite + spalte + 1}: {poraver_anteil_bereich:.2f}%")

        # Bereiche separat speichern
        bereichsnummer = zeile * anzahl_teilungen_breite + spalte + 1
        bereichsname = f"Bereich_{bereichsnummer}_Poraver_{poraver_anteil_bereich:.2f}%.png"
        vollstaendiger_pfad = os.path.join("C:/Haney/Studium/Master Arbeit/1_Python", bereichsname)

        # Speichern
        cv2.imwrite(vollstaendiger_pfad, bereich_mit_konturen)

```

```

poraver_anteile_liste.append(poraver_anteil_bereich)
df_poraver_anteile_liste.append({'Bereichsnummer': bereichsnummer, 'Poraver-Anteil (%)':
                                poraver_anteil_bereich})

plt.tight_layout()
plt.show()

# Excel-Datei speichern
excel_pfad = "C:/Haney/Studium/Master Arbeit/1_Python/Für Masterarbeit V2/Poraver_An-
             teile.xlsx"
df_poraver_anteile = pd.DataFrame(df_poraver_anteile_liste)
df_poraver_anteile.to_excel(excel_pfad, index=False, engine='openpyxl')

# Nachdem alle Poraver-Anteile berechnet wurden, führe die statistischen Berechnungen aus
mittelwert = np.mean(poraver_anteile_liste)
standardabweichung = np.std(poraver_anteile_liste)
cv = (standardabweichung / mittelwert) * 100

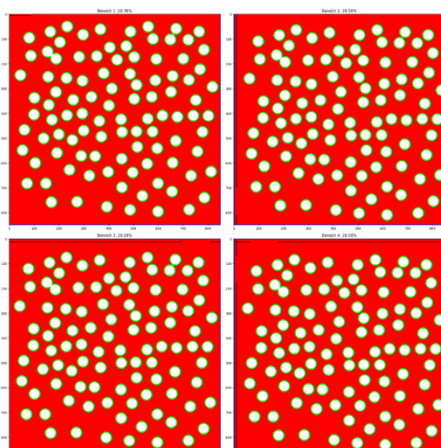
# Ausgabe der Ergebnisse
print(f"Mittelwert der Poraver-Anteile: {mittelwert:.2f}%")
print(f"Standardabweichung der Poraver-Anteile: {standardabweichung:.2f}%")
print(f"Variationskoeffizient der Poraver-Anteile: {cv:.2f}%")

```

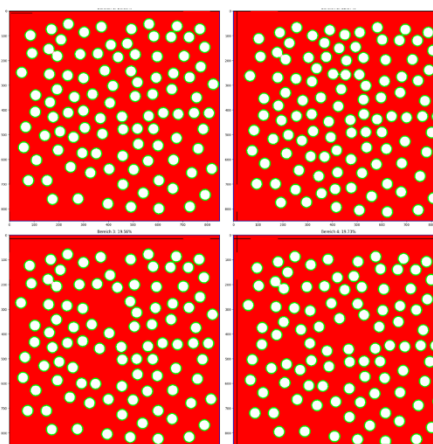
B Appendix

		Fall 1			Fall 2		
		Verteilung	Erwartete Wert	berechnete Wert	Verteilung	Erwartete Wert	berechnete Wert
Globale Poraveranteil		400	19,63	20,62	400	19,63	20,57
Bereich Poraveranteil	Bereich 1	100	19,63	20,76	100	19,63	20,59
	Bereich 2	100	19,63	20,56	109	21,40	22,37
	Bereich 3	100	19,63	20,59	95	18,65	19,56
	Bereich 4	100	19,63	20,58	96	18,85	19,73
Mittelwert			19,63	20,62		19,63	20,57
Standardabweichung			0	0,08		1,08	1,11
CV			0	0,37		5,52	5,41
		Fall 3			Fall 4		
		Verteilung	Erwartete Wert	berechnete Wert	Verteilung	Erwartete Wert	berechnete Wert
Globale Poraveranteil		400	19,63	20,57	400	19,63	20,72
Bereich Poraveranteil	Bereich 1	120	23,56	24,72	175	34,36	36,3
	Bereich 2	125	24,54	25,69	175	34,36	36,26
	Bereich 3	95	18,65	19,56	50	9,82	10,3
	Bereich 4	60	11,78	12,32	0	0,00	0
Mittelwert			19,63	20,57		19,63	20,72
Standardabweichung			5,05	5,3		15,13	15,99
CV			25,74	25,77		77,06	77,17

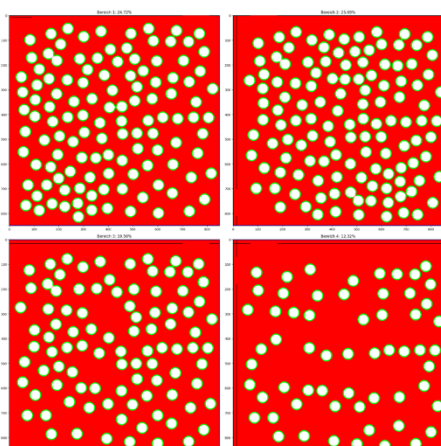
Fall 1: 100 % Homogen



Fall 2: geringe Variabilität



Fall 3: Moderate Variabilität



Fall 4: Hohe Variabilität

